

ASTB23 - Lecture 21

Relaxation in stellar systems

Relaxation and evolution of globular clusters

The virial theorem and the negative heat capacity of gravitational systems

Mass segregation, evaporation of clusters

Monte Carlo, N-body and other simulation methods

Why isn't galaxy bumpy?

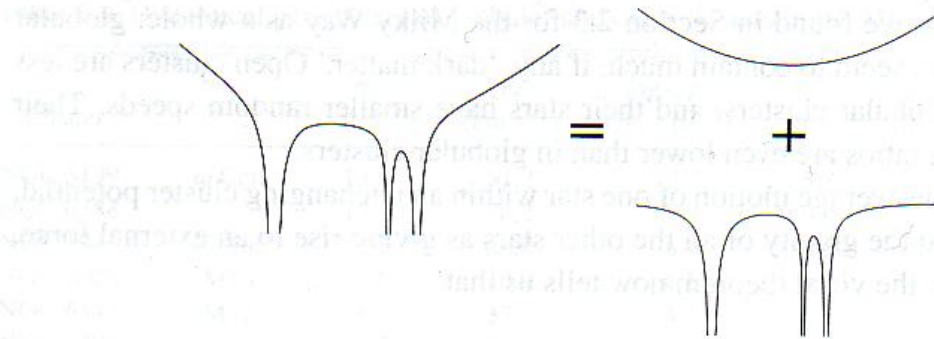


Figure 3.3 The potential $\Phi(\mathbf{x})$ of a stellar system, represented here by vertical height, can be split into a smoothly varying averaged component and a steep potential well near each star.

Similarly, we can think of the gravitational potential of the Galaxy as the sum of two parts: a smooth component, averaged over a region containing many stars, and the remainder, which includes the very deep potential well around each star (Figure 3.3). The successive tugs of individual stars on each other, described by the sharply varying part of the potential, cause them to deviate from the courses they would have taken if only the smooth part of the force had been present: we can think of these sharp pulls as 'collisions' between stars.

We will see in this section that stars in a galaxy behave quite differently from air molecules. The cumulative effect of the small pulls of distant stars is more important in changing the course of a star's motion than the huge forces generated as stars pass very near to each other. But except in dense star clusters, even these distant collisions have little effect over the lifetime of the Galaxy in randomizing or 'relaxing' the stellar motions. For example, the smooth averaged part of the Galactic potential almost entirely determines the motion of stars like the Sun.

The physical collisions between stars are very very rare, but close approaches are more frequent. We call them "collisions".

3.2.1 Strong close encounters

We can calculate the average time between strong encounters, in which one star comes so near to another that the collision completely changes its speed and direction of motion, as follows. Suppose the stars all have mass m and move in random directions with average speed V . For the moment, we neglect the gravitational force from the rest of the galaxy or cluster. Then if two stars approach within a distance r , the sum of their kinetic energies must increase to balance the change in potential energy. When they are a long way apart, their mutual potential energy is zero. We say that they have a *strong encounter* if, at their closest approach, the change in potential energy is at least as great as their starting kinetic energy. This requires

$$\frac{Gm^2}{r} \gtrsim \frac{mV^2}{2}, \quad \text{which means} \quad r \lesssim r_s \equiv \frac{2Gm}{V^2}; \quad (3.46)$$

we call r_s the strong encounter radius. Near the Sun, stars have random speeds of $V \approx 30 \text{ km s}^{-1}$, and taking $m = 0.5M_\odot$ gives $r_s \approx 1 \text{ AU}$.

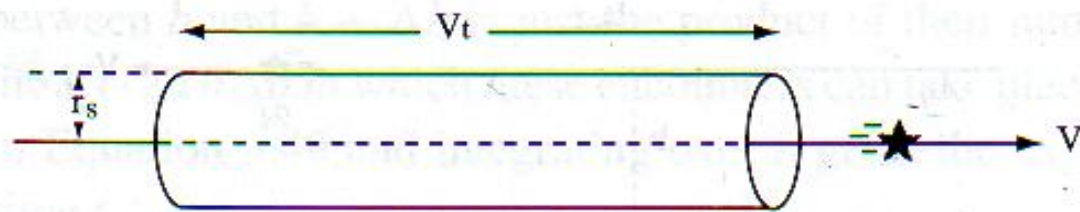


Figure 3.4 During time t , this star will have a strong encounter with any other star lying within the cylinder of radius r_s .

How often does this happen? We know that the Sun has not had a strong encounter in the past 4.5 Gyr; if another star had come so near, it would have disrupted the orbits of the planets. As the Sun moves relative to nearby stars at speed V for a time t , it has a strong encounter with any other stars within a cylinder of radius r_s , and volume $\pi r_s^2 V t$ centred on its path (see Figure 3.4). If there are n stars per unit volume, our Sun will on average have one close encounter in a time t_s such that $n\pi r_s^2 V t = 1$, so the mean time between strong encounters is

$$t_s = \frac{V^3}{4\pi G^2 m^2 n} \approx 4 \times 10^{12} \text{ yr} \left(\frac{V}{10 \text{ km s}^{-1}} \right)^3 \left(\frac{m}{\mathcal{M}_\odot} \right)^{-2} \left(\frac{n}{1 \text{ pc}^{-3}} \right)^{-1}. \quad (3.47)$$

$$t_s = \frac{V^3}{4\pi G^2 m^2 n} \approx 4 \times 10^{12} \text{ yr} \left(\frac{V}{10 \text{ km s}^{-1}} \right)^3 \left(\frac{m}{\mathcal{M}_\odot} \right)^{-2} \left(\frac{n}{1 \text{ pc}^{-3}} \right)^{-1}. \quad (3.47)$$

In Section 2.1 we found that $n \approx 0.1 \text{ pc}^{-3}$ for stars near the Sun; so $t_s \sim 10^{15}$ years. This is about ten million ‘Galactic years’, and it far exceeds the age of the Universe. Gravity is a much weaker force than the electromagnetic forces between atoms, and even though stars are by terrestrial standards very massive, they still do not often come close enough for the gravitational attraction of one to cause a large change in another’s orbit. Strong encounters are important only in the dense cores of globular clusters, and in galactic nuclei.

3.2.2 Distant weak encounters

For molecules in the air, the electric and magnetic forces of distant particles will tend to cancel each other, averaging to zero. Thus strong close encounters are overwhelmingly more important in changing their speeds and direction of motion. But gravity is always an attractive force; a star is pulled toward all other stars, however far away. In this section we will see that the cumulative pull of distant stars is more effective over time in changing a star’s direction of motion than are single close encounters.

In a distant encounter, the force of one star on another is so weak that the stars hardly deviate from their original paths while the encounter takes place. So we can use the *impulse approximation*, calculating the forces that the stars would feel as they move along the paths they would follow if they had not been disturbed. We start with a star of mass \mathcal{M} , moving at speed V along a path that will take it within distance b of a stationary star of mass m (Figure 3.5). The motion of \mathcal{M} is approximately along a straight line; the pull of m gives it a small motion V_{\perp} perpendicular to that path. If we measure time from the point of closest approach,

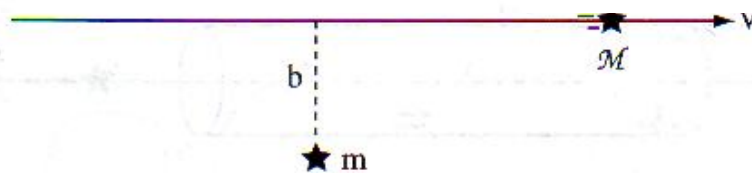


Figure 3.5 A weak encounter: star \mathcal{M} moves at speed V past the stationary star m , approaching to within distance b .

the perpendicular force is

$$\mathbf{F}_{\perp} = \frac{Gm\mathcal{M}b}{(b^2 + V^2t^2)^{3/2}} = \mathcal{M} \frac{dV_{\perp}}{dt}. \quad (3.48)$$

Integrating over time, we find that long after the encounter, the perpendicular speed of \mathcal{M} is

$$\Delta V_{\perp} = \frac{1}{\mathcal{M}} \int_{-\infty}^{\infty} \mathbf{F}_{\perp}(t) dt = \frac{2Gm}{bV}; \quad (3.49)$$

the faster \mathcal{M} flies past m , the smaller the velocity change. In this approximation,

forward at times $t < 0$ exactly balances that pulling it back when $t > 0$. So the path of \mathcal{M} is bent through an angle

$$\alpha = \frac{\Delta V_{\perp}}{V} = \frac{2Gm}{bV^2}. \quad (3.50)$$

Setting $V = c$ here shows that according to Newtonian gravity, light should be bent by exactly *half* the angle that general relativity predicts, in Equation 2.21.

Momentum in the direction of \mathbf{F}_{\perp} must be conserved, so after the encounter star m is moving toward the path of \mathcal{M} at a speed $2G\mathcal{M}/bV$. The impulse approximation is valid only if the perpendicular motion does not change the relative positions of \mathcal{M} and m significantly over the time $\Delta t \sim b/V$ during which most of the velocity change takes place. The perpendicular velocity of approach must be small compared with V , so we need

$$b \gg \frac{2G(m + \mathcal{M})}{V^2}. \quad (3.51)$$

Thus a weak encounter requires b to be much larger than r_s , the strong encounter radius of Equation 3.46.

As star \mathcal{M} proceeds through the Galaxy, many stars m will tug at it, each changing its motion by an amount ΔV_{\perp} , but in different directions. If the forces are random, then we should add the squares of the perpendicular velocities to find the expected value of ΔV_{\perp}^2 . During time t , the number of stars m passing \mathcal{M} with

separations between b and $b + \Delta b$ is just the product of their number density n and the volume $Vt \cdot 2\pi b \Delta b$ in which these encounters can take place. Multiplying by ΔV_{\perp}^2 from Equation 3.49 and integrating over b gives the expected squared speed: after time t ,

$$\langle \Delta V_{\perp}^2 \rangle = \int_{b_{\min}}^{b_{\max}} n V t \left(\frac{2Gm}{bV} \right)^2 2\pi b db = \frac{8\pi G^2 m^2 n t}{V} \ln \left(\frac{b_{\max}}{b_{\min}} \right). \quad (3.52)$$

After a time t_{relax} such that $\langle \Delta V_{\perp}^2 \rangle = V^2$, the star's expected speed perpendicular to its original path becomes roughly equal to its original forward speed; the 'memory' of its initial path has been lost. Defining $\Lambda \equiv (b_{\max}/b_{\min})$, we find that this relaxation time is much shorter than the strong encounter time t_s of Equation 3.47:

$$t_{\text{relax}} = \frac{V^3}{8\pi G^2 m^2 n \ln \Lambda} = \frac{t_s}{2 \ln \Lambda} \\ \approx \frac{2 \times 10^9 \text{ yr}}{\ln \Lambda} \left(\frac{V}{10 \text{ km s}^{-1}} \right)^3 \left(\frac{m}{\mathcal{M}_{\odot}} \right)^{-2} \left(\frac{n}{10^3 \text{ pc}^{-3}} \right)^{-1}. \quad (3.53)$$

It is not clear what value we should take for Λ . Our derivation is certainly not valid if $b < r_s$, and we usually take $b_{\min} = r_s$, and b_{\max} as equal to

In an isolated cluster consisting of N stars with mass m moving at average speed V , the average separation between stars is roughly half the size R of the system. Equation 3.42 then tells us that

$$\frac{1}{2}NmV^2 \sim \frac{G(Nm)^2}{2R}, \quad \text{so } \Lambda = \frac{R}{r_s} \sim \frac{GmN}{V^2} \cdot \frac{V^2}{2Gm} \sim \frac{N}{2}. \quad (3.54)$$

The crossing time $t_{\text{cross}} \sim R/V$; since $N = 4n\pi R^3/3$, we have

See book's errata

$$\frac{t_{\text{relax}}}{t_{\text{cross}}} \sim \frac{\frac{1}{6} V^4 R^2}{NG^2 m^2 \ln \Lambda} \sim \frac{N}{6 \ln(N/2)}. \quad (3.55)$$

In a galaxy with $N \sim 10^{11}$ stars, relaxation will be important only after about 10^8 crossing times, much longer than the age of the Universe. Globular clusters contain about 10^6 stars, so for the cluster as a whole $t_{\text{relax}} \sim 10^4 t_{\text{cross}} \sim \underline{10^{10} \text{ yr}}$. In an open cluster with $N = 100$, as we saw above, the two timescales are almost equal.

Computer simulations of galaxies generally use between 10^4 and 10^6 'stars' attracting each other by their gravity, according to Equation 3.2. Galaxies are centrally concentrated, and in the dense inner regions, crossing times are only 10^6 – 10^7 years. Equation 3.55 shows that if the 'stars' are treated as point masses, particles are pulled right off their original orbits on timescales $t_{\text{relax}} \lesssim 10^3 t_{\text{cross}} \sim \underline{10^{10} \text{ yr}}$. These computations cannot be trusted to behave like a real galaxy for longer than a gigayear or two; beyond that, relaxation is important. We can extend

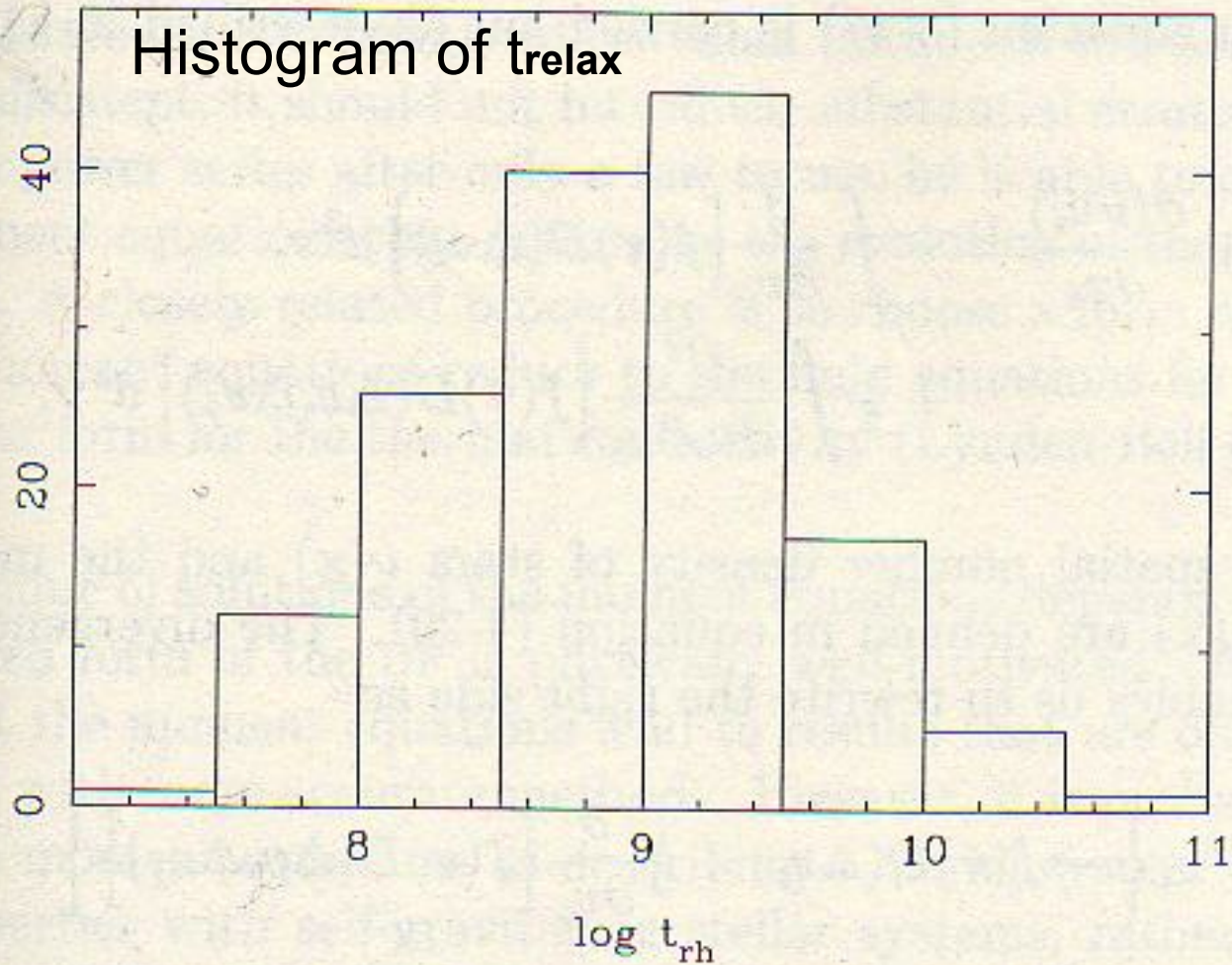


Figure 8-2. The distribution of median relaxation time t_{rh} in years for 147 galactic globular clusters. The results are based on the tabulation of Webbink (1985), assuming a stellar mass $m = 0.7 M_{\odot}$ and mass-to-light ratio $\Upsilon = 2\Upsilon_{\odot}$.

Relaxation effects in real systems: in globular clusters

$$t_{rlx} = 10^5 - 10^6 \text{ yr}$$

3.2.3 Effects of two-body relaxation

While a star moves in the smoothed potential of a star cluster, its orbit does not depend on whether it is heavy or light, but only on its position or velocity. If the smoothed potential $\Phi(\mathbf{x})$ does not change with time, Equation 3.25 tells us that the energy of the star remains constant. By contrast, two-body ‘collisions’ allow two stars to exchange energy and momentum in a way that depends on both their masses; this is known as *two-body relaxation*.

Just as for the air molecules in a room, the exchanges on average will shift the velocities of the stars toward the most probable way of sharing the available energy: this is a Maxwellian distribution. The fraction f of stars with velocities v between v and $v + \Delta v$ is given by $f_M(\mathcal{E}) 4\pi v^2 \Delta v$, where

$$f_M(\mathcal{E}) \propto \exp\{-\mathcal{E}/k_B T\} = \exp\left\{-\left[m\Phi(\mathbf{x}) + \frac{mv^2}{2}\right]/k_B T\right\}; \quad (3.56)$$

k_B is Boltzmann’s constant. The ‘temperature’ T depends on the energy of the system: the faster the stars are moving, the higher is T . By integrating $v^2 f_M(\mathcal{E})$ over velocity (see Section 3.3 below, or a text on statistical mechanics), we find that for stars of mass m , T is related to the average of the squared velocities by

$$\frac{1}{2}m\langle v^2(\mathbf{x}) \rangle = \frac{3}{2}k_B T. \quad (3.57)$$

The virial theorem (p. ~105 of textbook)

refers to time averages of energies in a system in **equilibrium**:

E_{kin} = total kinetic energy = sum of all $\frac{1}{2} mv^2$

E_{pot} = total potential energy

E = total mechanical energy = $E_{\text{kin}} + E_{\text{pot}}$

Virial theorem:

$$2E_{\text{kin}} + E_{\text{pot}} = 0$$

$$2(E - E_{\text{pot}}) + E_{\text{pot}} = 0 \quad \Rightarrow \quad E_{\text{pot}} = 2E$$

$$\text{also} \quad E_{\text{kin}} = -E$$

Mnemonic: using, as we almost always do, E as specific energy (en. per unit mass of test particle), the circular Keplerian motion has Keplerian circular speed v , where

$v^2 = GM/r$ (derived from acceleration eq.: $v^2/r = GM/r^2$), thus

$E_{\text{kin}} = \frac{1}{2} v^2 = \frac{1}{2} GM/r$ (kin. en. per unit mass)

$E_{\text{pot}} = -GM/r$ (pot. en. per unit mass)

$E = -\frac{1}{2} GM/r$

thus $E_{\text{pot}} = 2E$, $E_{\text{kin}} = -E$, and $2E_{\text{kin}} = -E_{\text{pot}}$, i.e. virial relations!

One interesting consequence of the Virial Theorem:

As you know, temperature is just a rescaled thermal (kinetic) energy:

$$E_{\text{kin}} = \frac{1}{2} N m \langle v^2 \rangle = \frac{3}{2} N k_B T \quad (\text{gas of } N \text{ atoms, molecules, stars,...})$$

According to the Virial Theorem, $E = - E_{\text{kin}}$, so

$$dE/dT = -(3/2) N k_B < \mathbf{0}$$

We call dE/dT the specific heat in thermodynamics.

In gravitationally bound systems, specific heat is negative.

Removing energy from the system makes it hotter (i.e. higher T)!

We've seen this seeming paradox inside stars and gas clouds, too. It's due to the gravity being always attractive: the potential wells are negative-valued. Sinking into them leads to faster motions → hotter system of particles, not colder like in laboratory thermodynamics, where potentials are positive.

These stars leave the cluster; but after a time t_{relax} , new stars are promoted to these high energies, and escape in their turn. The cluster loses a substantial fraction of its stars over an *evaporation time*

$$t_{\text{evap}} \sim 136t_{\text{relax}}. \quad (3.60)$$

In the observed globular clusters, t_{evap} is longer than the age of the Universe; any clusters with very short evaporation times presumably dissolved before we could observe them. For open clusters t_{evap} is only a few gigayears. In practice, these clusters fall apart even more rapidly, as evaporation is helped along by the repeated gravitational tugs of the giant molecular gas clouds in the Galactic disk, and of matter in the spiral arms.

Two-body relaxation also leads to mass segregation: heavier stars congregate at the cluster center, while lighter stars are expelled toward the periphery. If initially the cluster stars are thoroughly mixed, with similar orbital speeds, the more massive stars will have larger kinetic energy. But in a Maxwellian distribution, their average kinetic energies are equal. Thus on average, a massive star will be moving slower after a 'collision' than it did before. It then sinks to an orbit of lower energy; the cluster center fills up with stars that have too little energy to go anywhere else. As the cluster becomes centrally concentrated, these tightly bound stars must move faster than those further out, increasing their tendency to give up energy.

Meanwhile, the upwardly mobile lighter stars have gained energy from their encounters, but spend it in moving out to the suburbs. Their new orbits require slower motion than before, so they have become even poorer in kinetic energy. Mass segregation is a runaway process: the lightest stars are pushed outward into an ever-expanding diffuse outer halo, while the heavier stars form an increasingly dense core at the center. Pairs of stars bound in a tight binary will effectively behave like a single more-massive star, sinking to the core. The X-ray sources in globular clusters are binaries in which a main-sequence star orbits a white dwarf or neutron star; they are all found near the cluster center.

In a globular cluster, stars exceeding the escape speed v_{esc} leave the system, or "evaporate".

That's consequence #1 of relaxation-driven evolution.

Consequence #2 is the formation of gradually more compact and dense core.

Small, dense cores in globular clusters M15 and M4.

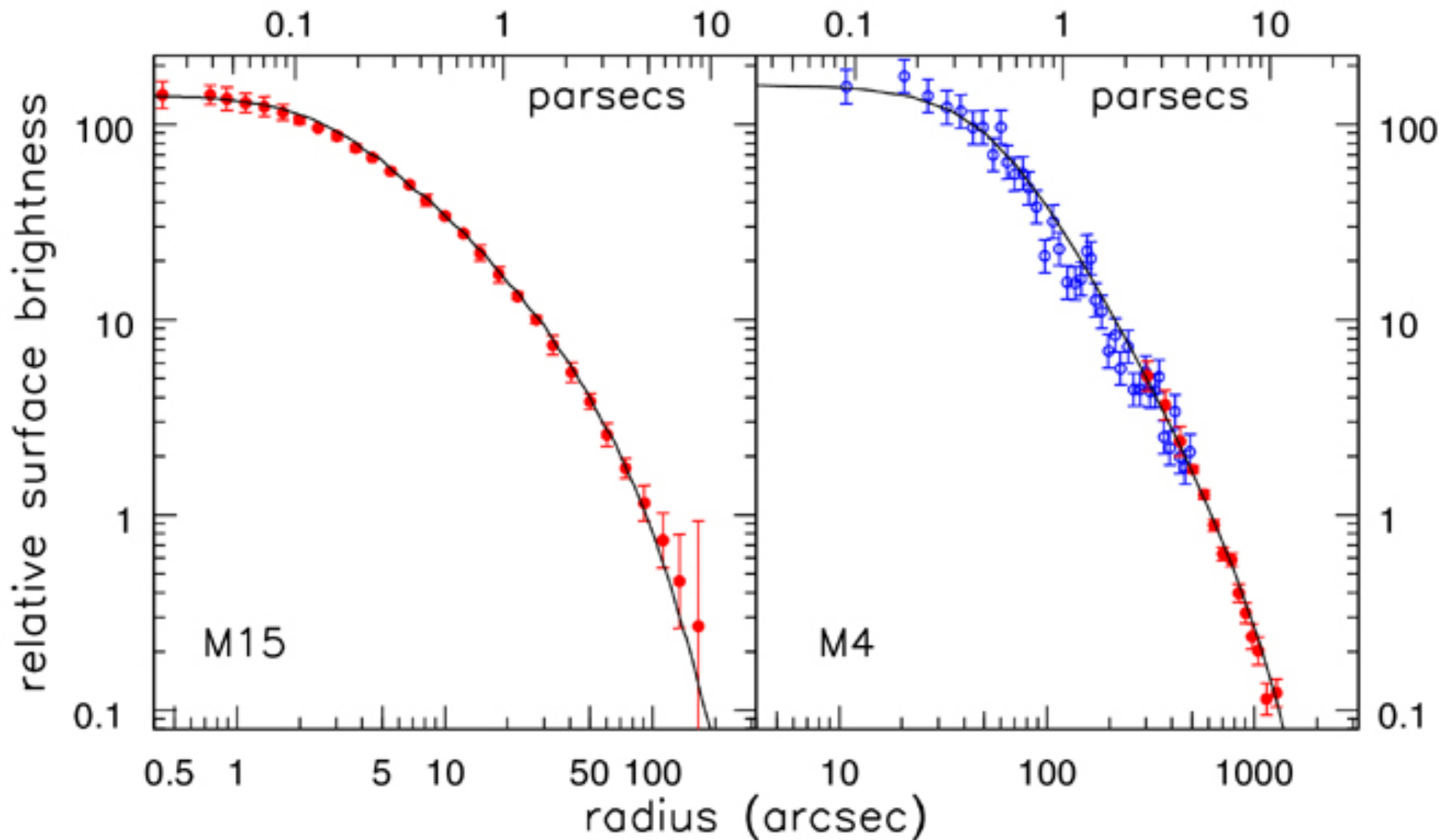


Fig 3.7 (Pasquali, Fahlman, Pryor) 'Galaxies in the Universe' Sparke/Gallagher CUP 2007

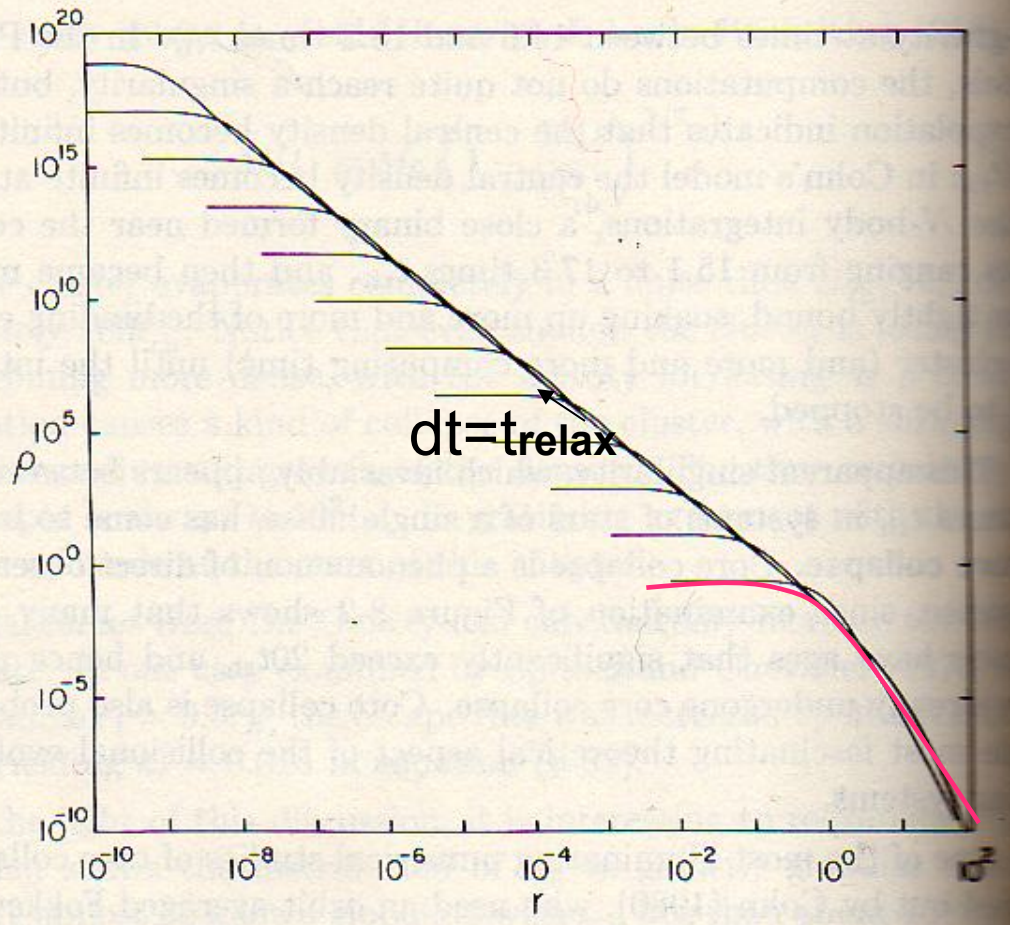
Evolution of a globular cluster

Results of a semi-analytic method using the so-called Fokker-Planck equation.

Unlike the Monte Carlo method, these results are not subject to statistical noise.

Typical time of evolution before *core collapse* is $20 t_{\text{relax}}$.

Core collapse is the name for extreme compactification of the stellar system's core.



The red, initial density profile
 $\rho \sim [1 + (r/b)^2]^{-1}$ or a similar, so-called, King model

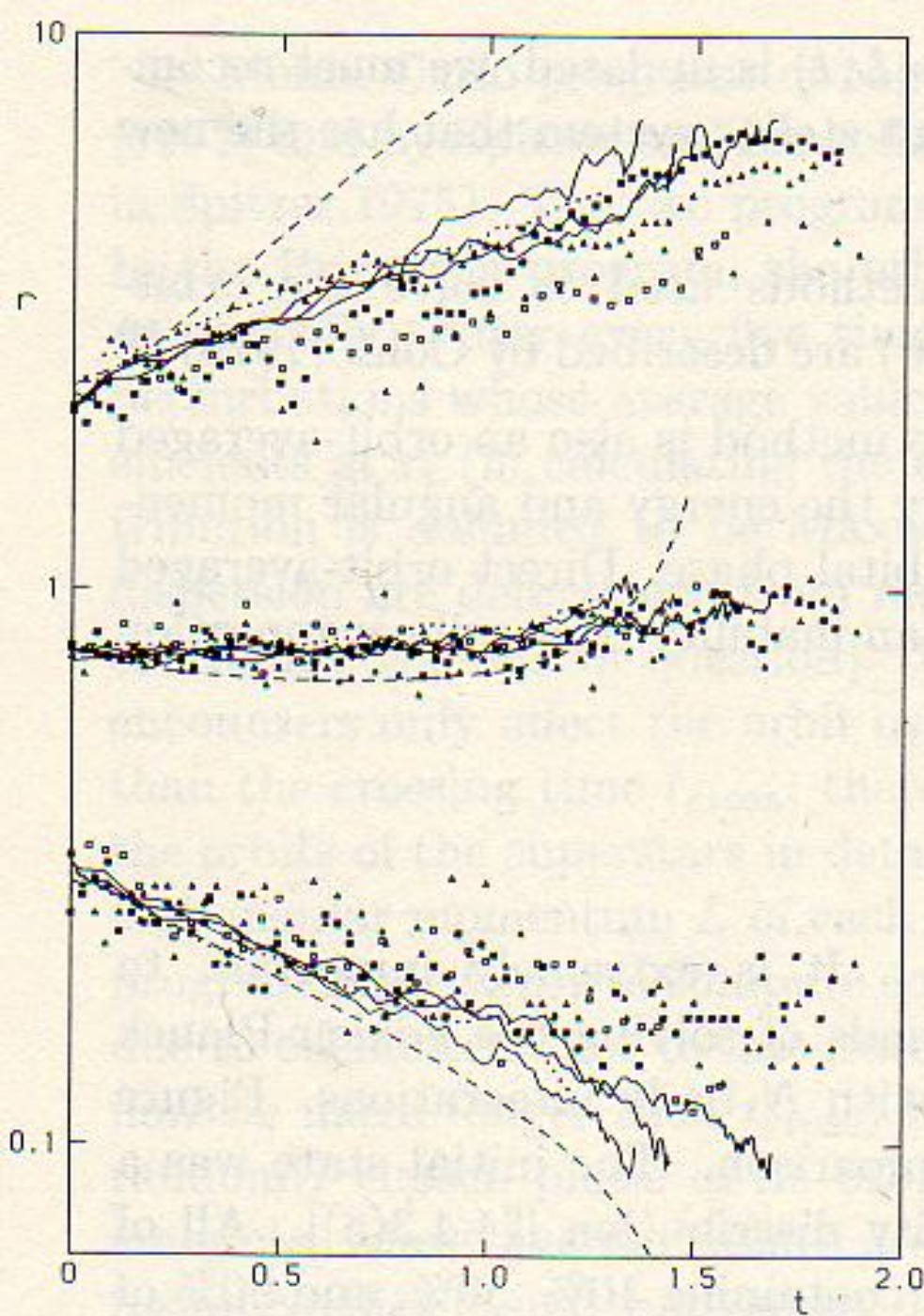
Evolution of a globular cluster

Initial profile was a Plummer sphere.

Comparison of results of a exact **N-body simulations (symbols)**, usually with $N=150-350$, with semi-analytic **Mte Carlo method (line)**.

In Mte Carlo method, stellar orbits in a smooth potential are followed with occasional added jolts simulating the weak and strong encounters. Random number generators help to randomize perturbations. The results are subject to significant statistical noise.

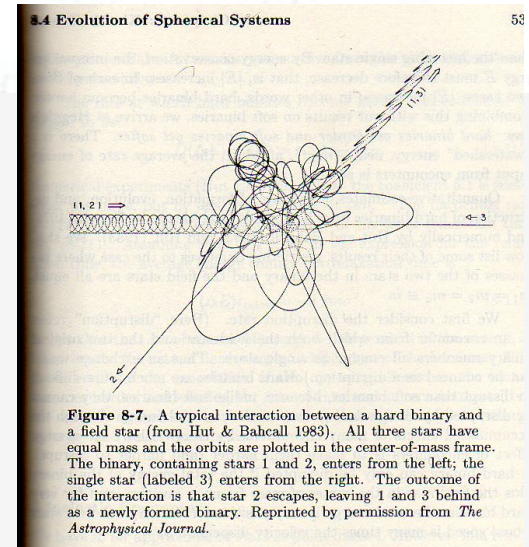
Upper lines show radius enclosing 90% of mass, middle lines 50%, and the lower show 10% of total mass.



core collapse (suspected also in M15, but not common)

stars predict that after $12\text{--}20 t_{\text{relax}}$, the core radius shrinks to zero, as the central density increases without limit: this is core collapse. A cluster that is near this state should have a small dense core, and a diffuse halo, as we see for NGC 6293 in Figure 3.6.

What happens to a cluster after core collapse? In the dense core, binary stars become important sources of energy. Just as two-body ‘collisions’ tend to remove energy from fast-moving stars, so encounters between single stars and a tight binary pair will on average take energy from the binary. The energy is transferred to the single star, while the binary is forced closer. Depending on how many are present, binaries may supply so much energy to the stars around them that the core of the cluster starts to re-expand.



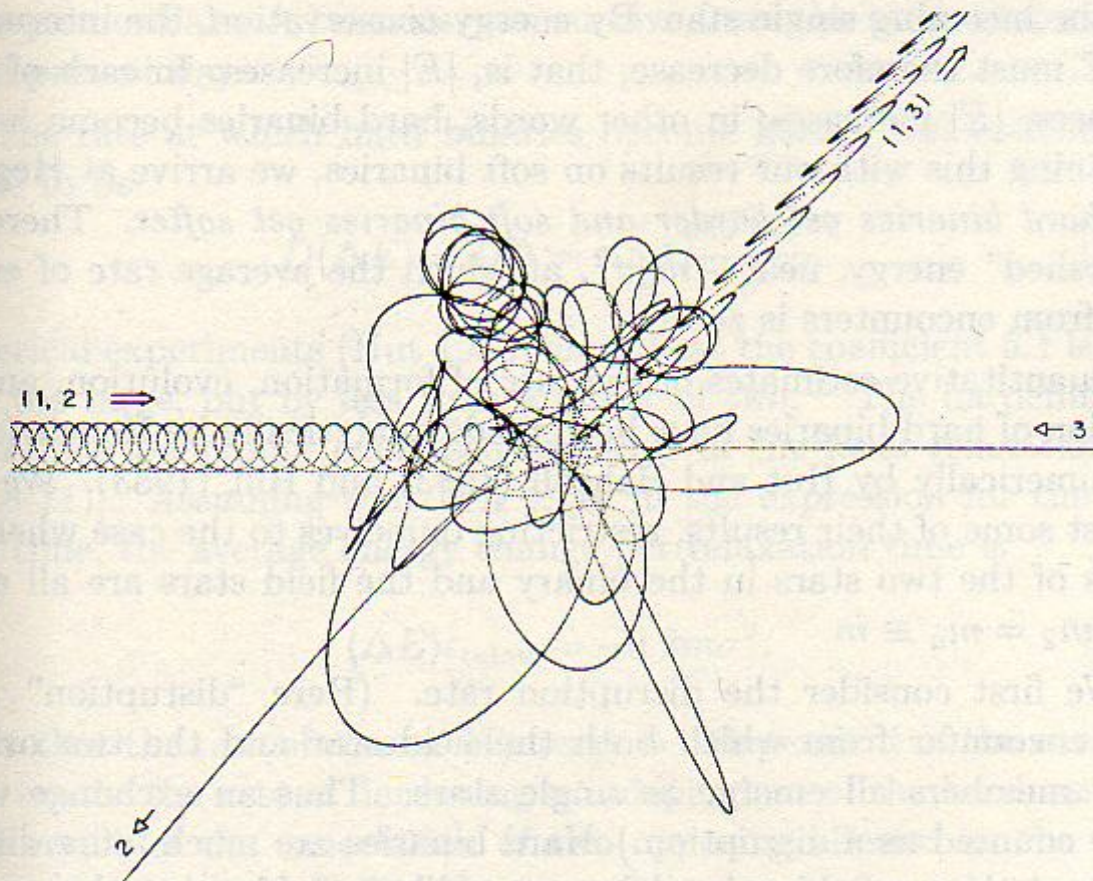


Figure 8-7. A typical interaction between a hard binary and a field star (from Hut & Bahcall 1983). All three stars have equal mass and the orbits are plotted in the center-of-mass frame. The binary, containing stars 1 and 2, enters from the left; the single star (labeled 3) enters from the right. The outcome of the interaction is that star 2 escapes, leaving 1 and 3 behind as a newly formed binary. Reprinted by permission from *The Astrophysical Journal*.

3-body interaction

a binary comes
from the left

encounters a single

and the components
trade places

ASTB23 - Lecture 22

Milky Way's kinematics and structure

Parallax and distance measurement

Luminosity and mass functions - a few basic facts

Kinematics of the solar neighborhood

Thin disk, thick disk

Open and globular clusters

- metallicity, age, distribution, motion

Infrared view

Galactic bulge and center

Rotation

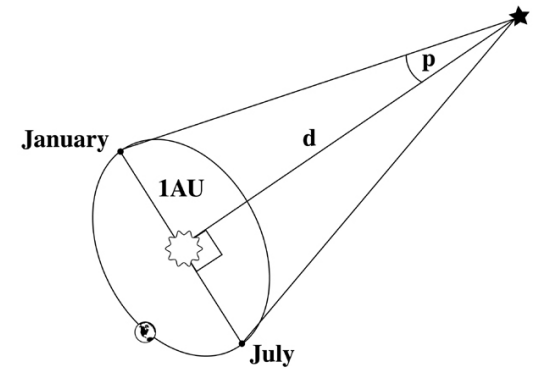


Fig 2.1 'Galaxies in the Universe' Sparke/Gallagher CUP 2007

Step number one:

Measure the parallax (the Hipparcos satellite, 1989-1993)

Measure the apparent magnitude m .

This could be done for 0.12 mln bright stars,

with positional accuracy \sim milliarcsec (1 milliarcsec = $1^\circ/3600000$)

Step number two:

Derive distance from $(d / 1\text{pc}) = (1'' / \text{parallax})$

Derive the absolute magnitude M from distance modulus

$m - M = 5 \log (d/10\text{pc}) = 5 \log (0.1'' / \text{parallax})$.

Knowing M for certain classes of stars gave accurate distances to a few hundred pc.

The most numerous stars in the Galaxy have mass 0.3-0.5 M_{sun}

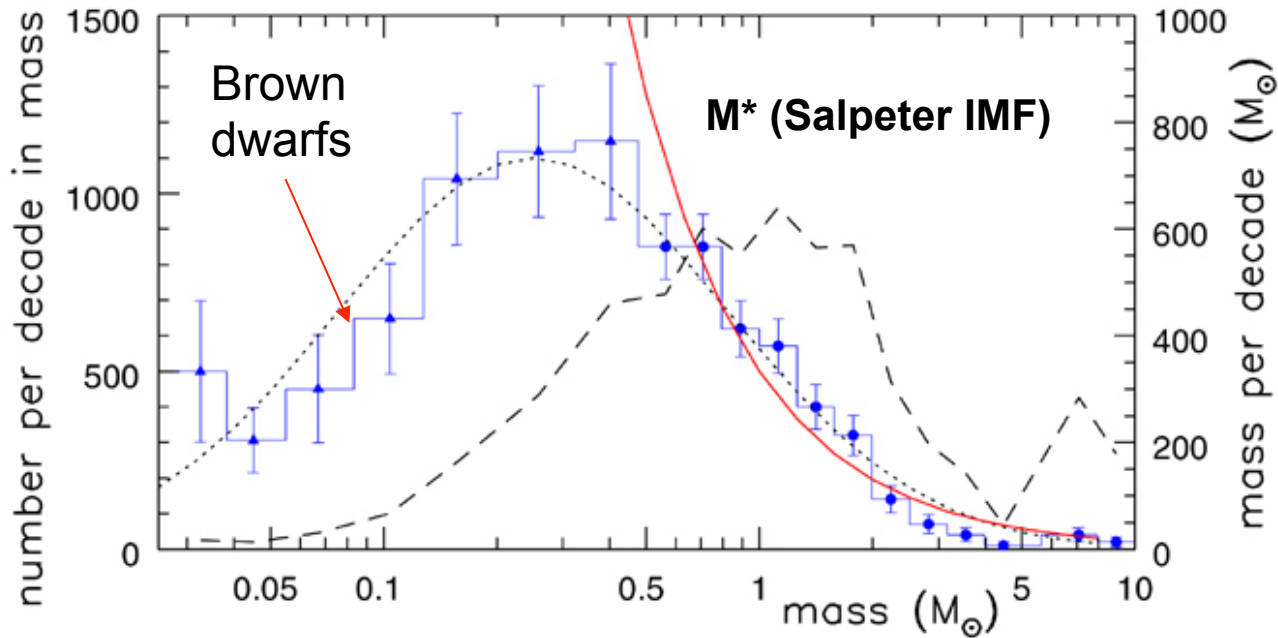


Fig 2.5 (E. Moreau) 'Galaxies in the Universe' Sparke/Gallagher CUP 2007

Frequency of stars with different masses = a power-law with exponent (index) -2.35

Near the Sun, we find roughly

$$\xi(M) = \xi_0 M^{-2.35}, \quad (2.5)$$

where the constant ξ_0 sets the local stellar density; this is called the *Salpeter IMF*. Figure 2.5 shows the observed numbers of stars at each mass in the Pleiades cluster, shown in Figure 2.10 below. This cluster is only 100 Myr old, so for masses

Using the Galaxy-centred spherical polar coordinates R, ϕ, z that were introduced in Section 1.2, we often approximate the density $n(R, z, S)$ of stars of a particular type S by a double exponential form,

$$n(R, z, S) = n(0, 0, S) \exp[-R/h_R(S)] \exp[-|z|/h_z(S)], \quad (2.8)$$

where h_R is called the *scale length* of the disk and h_z is the *scale height*. Figure 2.7 shows that near the midplane, $h_z \approx 300\text{--}350$ pc for K dwarfs, while for more massive and shorter-lived stars, such as the A dwarfs, it is smaller, $h_z \lesssim 200$ pc.

Thin and thick disks of the Galaxy

63

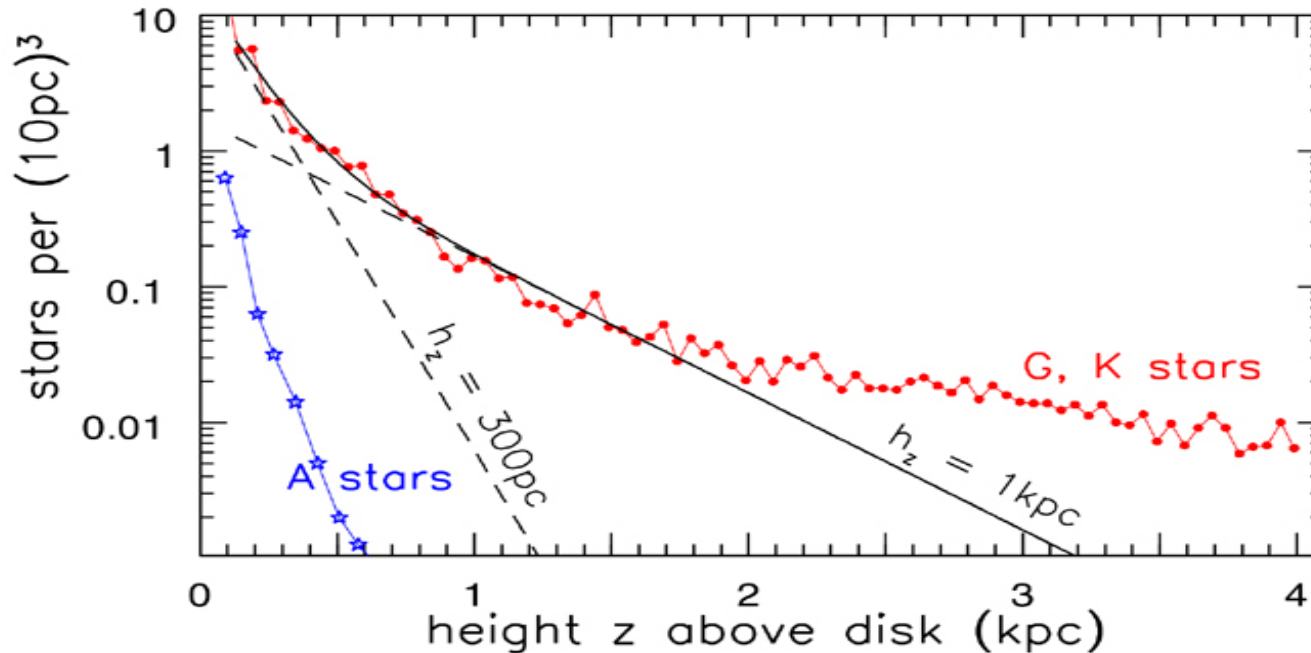


Fig 2.8 (Reid, Knude) 'Galaxies in the Universe' Sparke/Gallagher CUP 2007

Figure 2.7 Looking toward the south Galactic pole, filled circles show the density of stars with $5 < M_V < 6$; these are late G and early K dwarfs. Sloping dashed lines show $n(z) \propto \exp(-z/325 \text{ pc})$ (thin disk) and $n(z) \propto \exp(-z/1350 \text{ pc})$ (thick disk); the solid curve is their sum. At $z \gtrsim 2 \text{ kpc}$, most stars belong to the metal-poor halo. A dwarfs (star symbols) lie in a very thin layer – N. Reid, J. Knude.

Table 2.1 Scale heights and velocities of gas and stars in the disk and halo

<i>Galactic component</i>	h_z (pc)	σ_R (km s ⁻¹)	σ_ϕ (km s ⁻¹)	σ_z (km s ⁻¹)	$\langle v_y \rangle$ (km s ⁻¹)
HI gas near the Sun	130		≈5	≈7	tiny
Local CO, H ₂ gas	65		4		tiny
Disk stars: $Z > Z_\odot/4$		(Fig. 2.8)	small dispersion of velocity		
$\tau < 3$ Gyr	≈250	30	21	16	-11
$3 < \tau < 6$ Gyr	≈300	36	25	19	-9
$6 < \tau < 10$ Gyr	≈350	38	25	24	-16
$\tau > 10$ Gyr		62	52	37	-21
Thick disk			large dispersion of velocity		
$[\text{Fe}/\text{H}] > -0.8$	~1500	52	37	40	-35
Halo stars near Sun			huge dispersion of velocity		
$[\text{Fe}/\text{H}] < -1.6$	≥1 kpc	~150	~100	~100	-210
Halo stars at $2.5R_0$	few kpc	80–100	130–150	130–150	-220

Note: Gas velocities are measured looking up out of the disk (σ_z of HI), or at the tangent point (σ_ϕ for HI and CO); velocities of thin disk stars refer to F stars of Figure 2.8.

Velocity v_y is in the direction of Galactic rotation, relative to the *local standard of rest*, a circular orbit at the Sun's radius R_0 , assuming $v_{y,\odot} = 5 \text{ km s}^{-1}$.

This quantity measures the spread of vertical velocities v

$$\sigma_z^2 \equiv \langle v_z^2 - \langle v_z \rangle^2 \rangle,$$

Vertical velocity w.r.t. sun (W) as a function of stellar age: stars are born in a thin disk with small W ; older stars are in a thicker disk

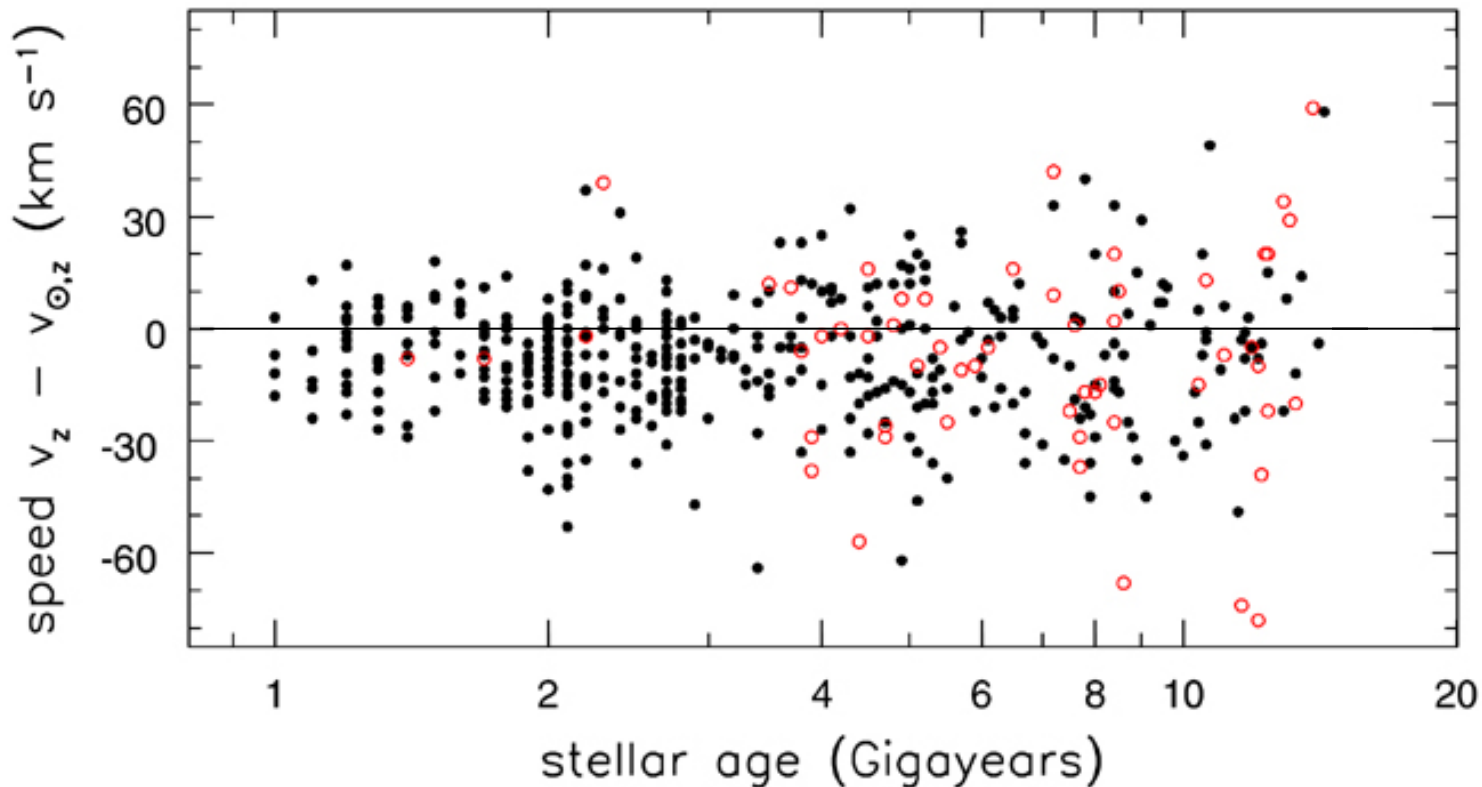


Fig 2.9 'Galaxies in the Universe' Sparke/Gallagher CUP 2007

Figure 2.8 For nearby main-sequence F stars, velocity $v_z - v_{z,\odot}$ is perpendicular to the Galactic plane, measured relative to the Sun. Open circles show stars with less than 1/4 of the Sun's iron abundance. Older stars tend to be moving faster; the average velocity is negative, showing that the Sun moves 'upward' at $7-8 \text{ km s}^{-1}$ – B. Edvardsson *et al.*, A&A 275, 101; 1993.

Vertical velocity w.r.t. sun (W) as a function of stellar age: stars are born in a thin disk with small W; older stars are in a thicker disk

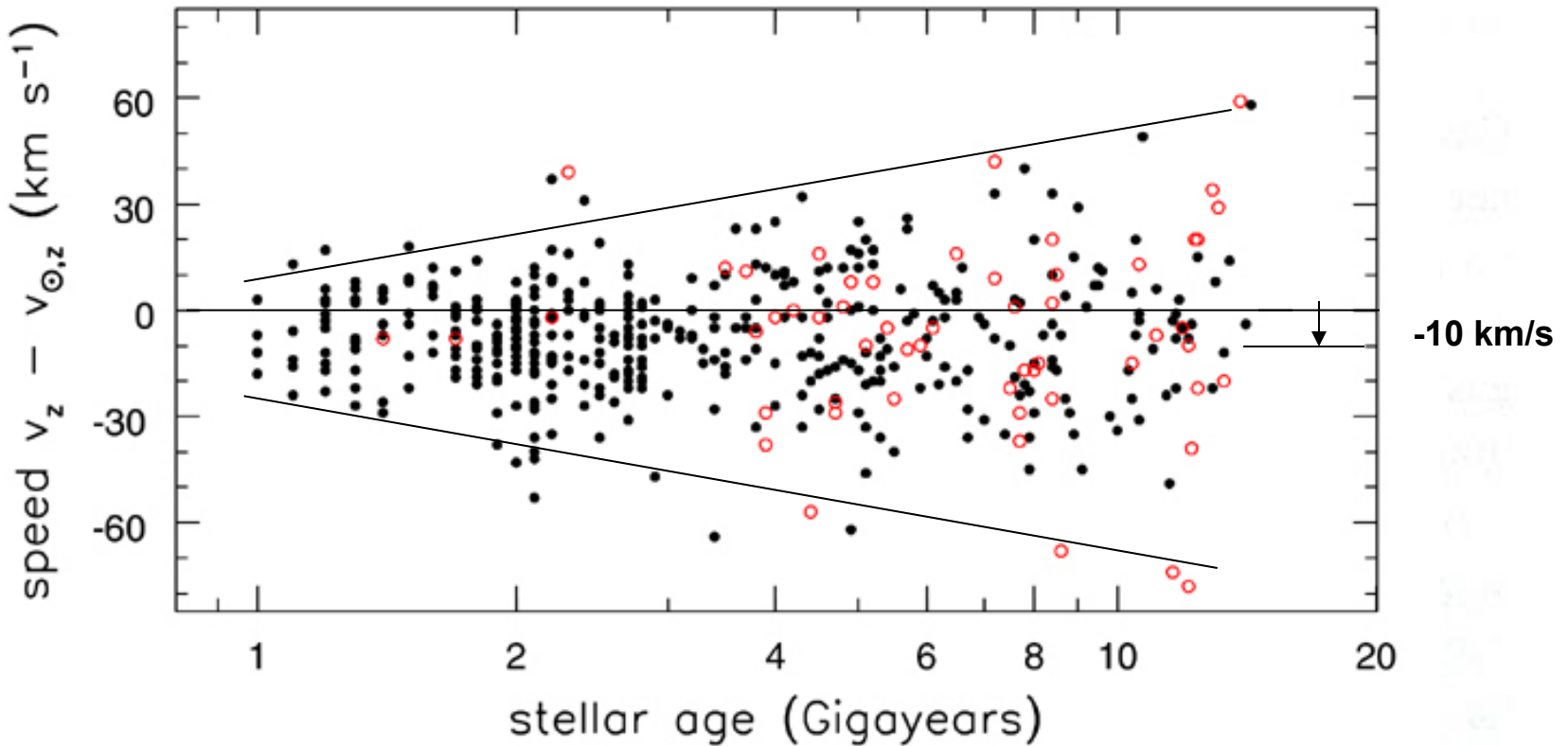


Fig 2.9 'Galaxies in the Universe' Sparke/Gallagher CUP 2007

Figure 2.8 For nearby main-sequence F stars, velocity $v_z - v_{z,\odot}$ is perpendicular to the Galactic plane, measured relative to the Sun. Open circles show stars with less than 1/4 of the Sun's iron abundance. Older stars tend to be moving faster; the average velocity is negative, showing that the Sun moves 'upward' at $7-8 \text{ km s}^{-1}$ – B. Edvardsson *et al.*, A&A 275, 101; 1993.

Open clusters - e.g., Pleiades, Hyades

(Pop I)

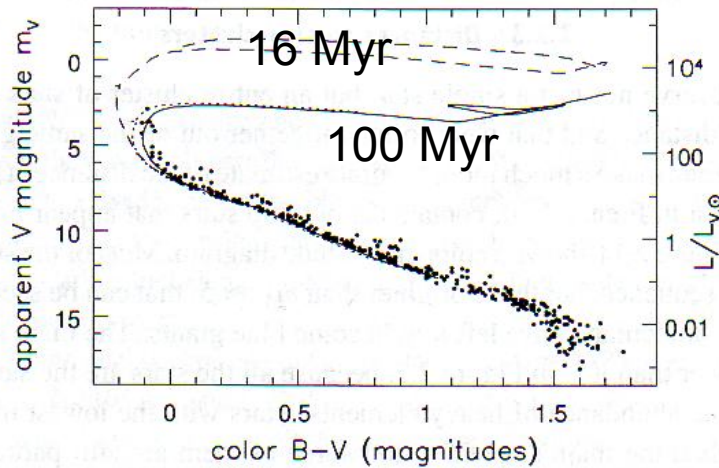


Figure 2.11 Measured apparent magnitude m_V and color $B - V$ for stars in cluster; points show observed stars, and the solid line is an isochrone for a old. The dotted line shows the same isochrone without correction for dust re dashed line is an isochrone for age 16 Myr – J.-C. Mermilliod.



Figure 2.10 Central region of the Pleiades open cluster; the brightest few stars easily outshine the rest of the cluster – NOAO.

Foreground
gas nebulae

Table 2.2 Some nearby open clusters

Cluster	d (pc)	$[Fe/H]$ ↓	M_V (mag)	L_V ($10^3 L_\odot$)	color ($B - V$)	r_c (pc)	σ_r (km s^{-1})	age (Myr)	
Pleiades	M45	130	0.11	-4.3	4.5	-0.05	1.5	$\lesssim 1$	100
NGC 6705	M11	1700	0.10	-6.1	24	0.17	0.7	1.2	200
Hyades		46	0.12	-2.7	1.0	0.40	2.7	0.3	625
NGC 2682	M67	870	-0.10	-3.3	2.4	0.65	1.1	0.6	4000

Note: d is the distance from the Sun; $[Fe/H] = \log_{10} Z/Z_\odot$; r_c is the core radius; and σ_r is the dispersion in the radial velocity V_r of stars in the cluster's central region.



47 Tucanae A large, bright globular cluster in the Milky Way, also known as NGC 104

47 Tucanae is the second brightest globular cluster. It contains ~1 mln star.

It can only be seen from the Southern Hemisphere.

This image is 34 arcmin across, ~0.56 degrees (comparable with Moon, Sun).

The infrared colors of all these stars are very similar.

Globular clusters - e.g. omega Centauri, 47 Tucanae

(Pop II)

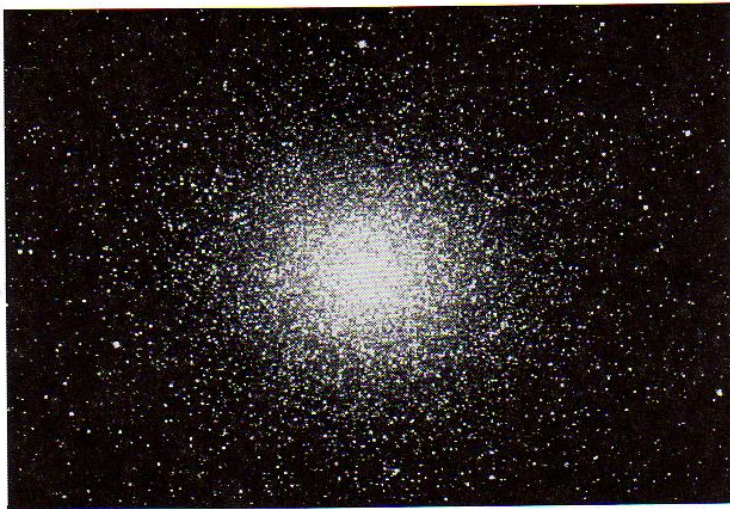


Figure 2.12 ω Centauri, the Milky Way's most luminous known globular cluster – V-band image from the CTIO Schmidt telescope.

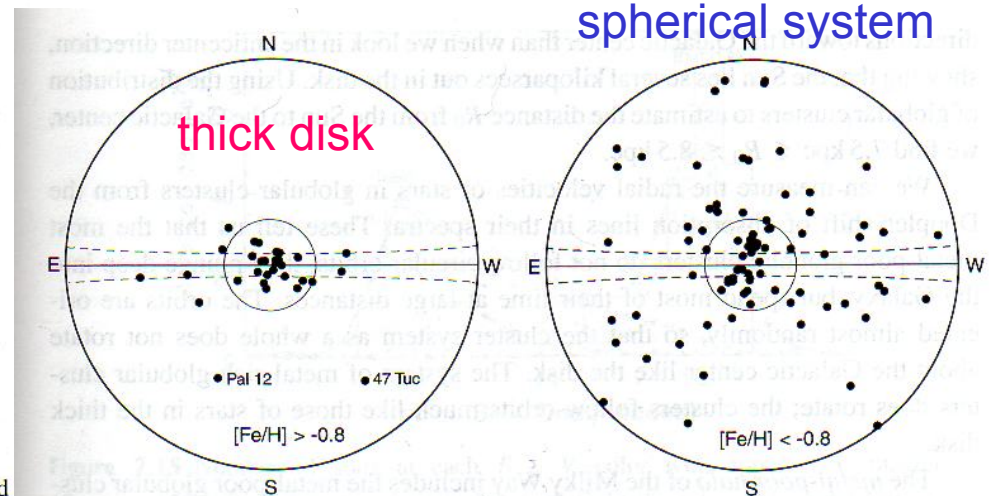


Figure 2.14 Positions projected on the sky, as seen from Earth, of metal-rich globular clusters (left), which lie close to the Milky Way's disk, and metal-poor clusters (right), with a more spherical distribution. The small circle marks 20° from the direction to the Galactic center; the large outer circle is at 90° ; the solid line is the Galactic equator. Between the dashed lines, at $b = \pm 5^\circ$, clusters may easily hide behind interstellar dust. 47 Tucanae is a nearby disk cluster, which is only 3 kpc from the Galactic plane; although metal rich, Palomar 12 is a halo cluster – R. Zinn.

Connection between *kinematics and geometry*: **thick disk** of high-metallicity globular clusters (left-hand panel) is made of objects on low-inclination, nearly-circular orbits \Leftrightarrow the system has some prograde rotation.

Spherical system (right panel) has completely disorganized motions, no rotation on average; some clusters have prograde, some retrograde motion; orbits are highly inclined. The same facts about rotation apply to individual stars in the Galaxy.

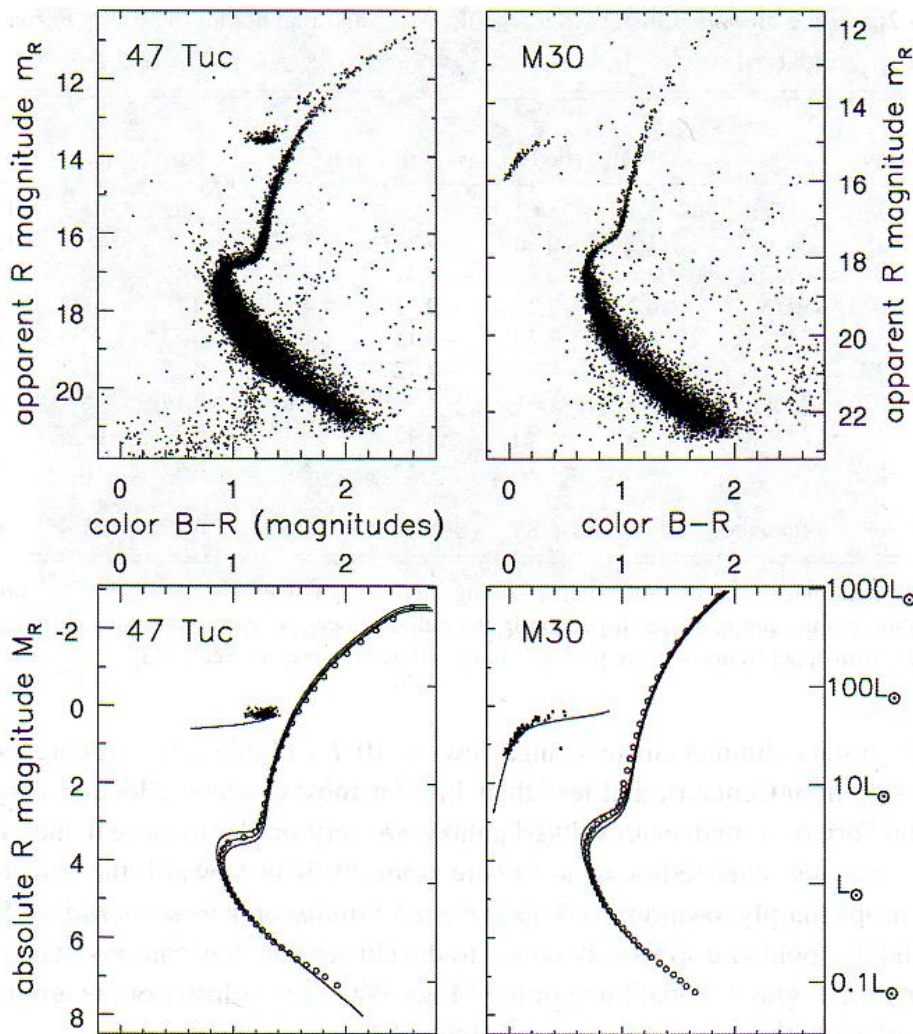


Figure 2.13 Above, color-magnitude diagrams for globular clusters 47 Tucanae and M30; all vertical scales coincide in absolute magnitude. Above left, the star sequence crossing the main sequence near $B - R, m_R = (1.25, 19.5)$ is the red giant branch of the Small Magellanic Cloud, seen in the background. Below, open circles show the central locus of the main sequence and red giants; solid curves are isochrones; a model zero-age horizontal branch is plotted along with the stars. Left, for 47 Tucanae, a metal-rich cluster, isochrones for $[Fe/H] = -0.83$, and ages of 10, 12, and 14 Gyr; right, for M30, a metal-poor cluster, isochrones with $[Fe/H] = -2.31$, and ages 12, 14, and 16 Gyr – T. Smecker-Hane.

Age, distance, metallicity are varied in models until the predicted H-R diagram (below) matches the observations (above).

For instance, 47 Tuc has $[Fe/H] = -0.83$ and age ~ 12 Gyr

Cluster M30 has fewer metals $[Fe/H] = -2.31$ and older age ~ 14 Gyr

One also uses RR Lyr variables (pulsating low-mass stars with $L \sim 50 L_{\odot}$) in glob. clusters as standard candles

INFRARED & RADIO VIEW of our GALAXY

SPECTRAL REGION	WAVELENGTH (microns)	TEMPERATURE (Kelvin)	WHAT WE SEE
Near-Infrared	0.8 to 5	740 to 5200	Cooler red stars, Red giants, Dust is transparent
Mid-Infrared	5 to 25	90 to 750	Planets, comets, asteroids Dust warmed by starlight Protoplanetary disks
Far-Infrared	25 to 350	10 to 100	Cold dust Central regions of galaxies Very cold molecular clouds
<hr/>			
Sub-mm and mm	850-2000	10 to 30	Larger (~mm), cold dust grains
Radio	e.g., 21 cm HI line		Global structure of the Galaxy, hydrogen clouds

Infrared view of the center of the Galaxy:

optical view

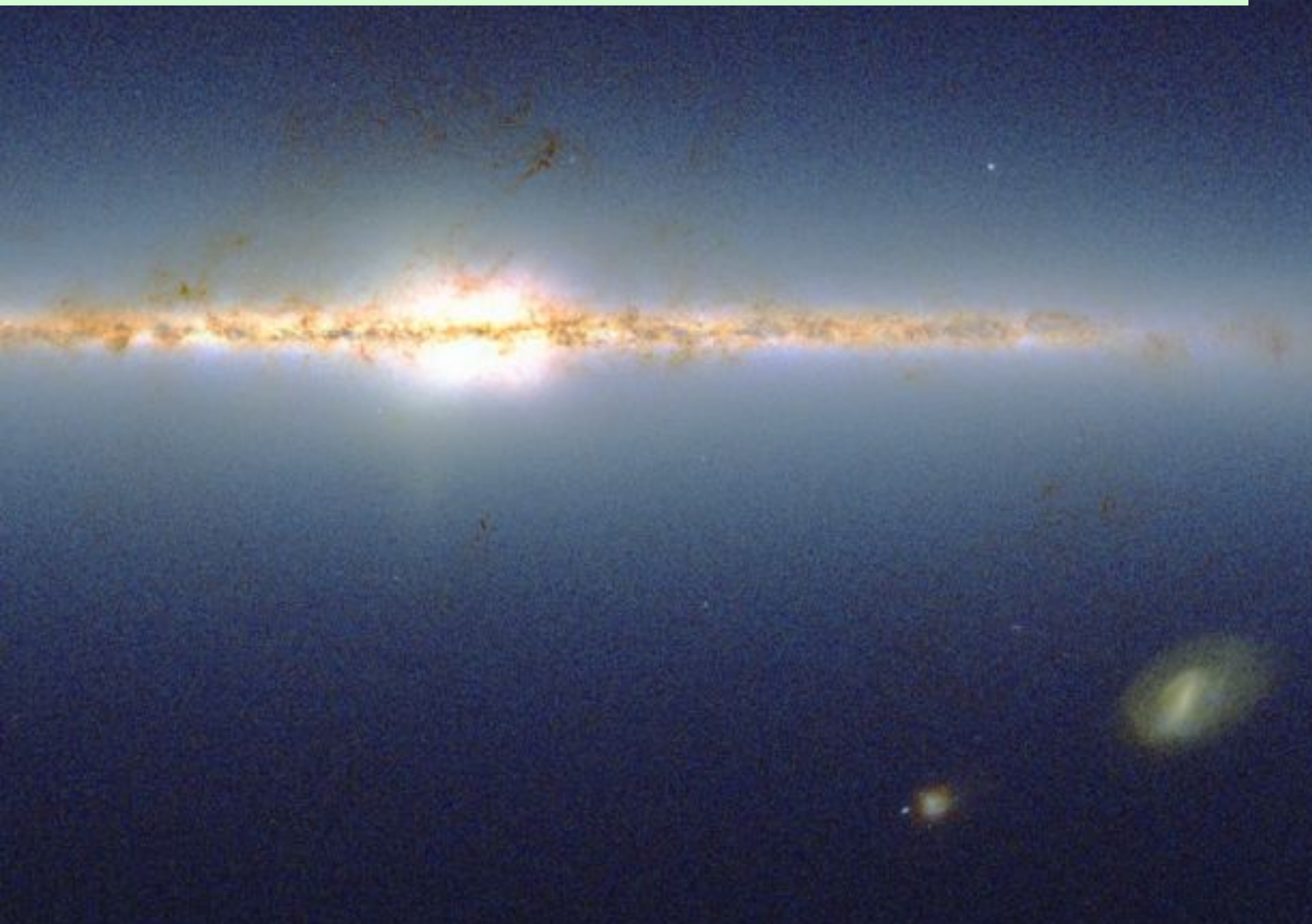


2MASS (2 micron all-sky) survey



Picture made from star counts
(not a direct image)
total of 250 mln stars measured
in 2MASS.

Infrared view of the Galaxy: 2MASS (2 micron all-sky) survey



Infrared view of the Galaxy

Using the Galaxy-centred spherical polar coordinates R, ϕ, z that were introduced in Section 1.2, we often approximate the density $n(R, z, S)$ of stars of a particular type S by a double exponential form,

$$n(R, z, S) = n(0, 0, S) \exp[-R/h_R(S)] \exp[-|z|/h_z(S)], \quad (2.8)$$

where h_R is called the *scale length* of the disk and h_z is the *scale height*. Figure 2.7 shows that near the midplane, $h_z \approx 300\text{--}350$ pc for K dwarfs, while for more massive and shorter-lived stars, such as the A dwarfs, it is smaller, $h_z \lesssim 200$ pc.

$h_R = 2$ to 4 kpc, both for the thin ($h_z \sim 0.3$ kpc) and the thick disk ($h_z \sim 1.5$ kpc)

Beyond $R=15$ kpc, the disk density is rapidly declining. The brightness distributions of other galaxies show similar downturns.

Infrared view of the Galaxy: 2MASS (2 micron all-sky) survey

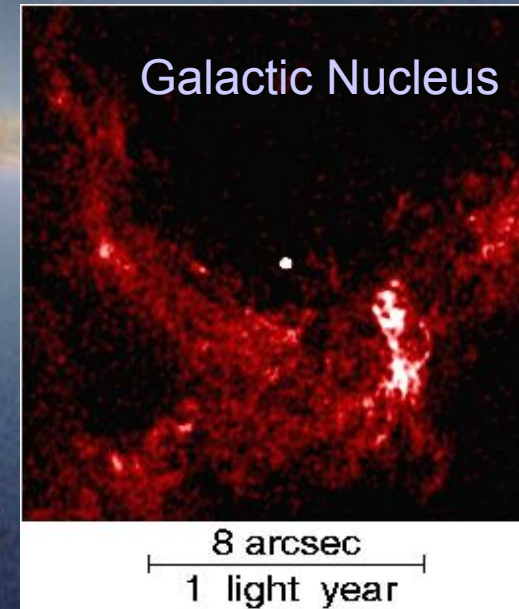
20% of Galaxy's light from the bulge, $R \sim 1$ kpc
Stars: few Gyr old, metal-rich unlike the metal-poor stars of the galactic halo, the inner halo is also more round and does not show rotation (bulge rotates in the prograde sense, like the sun, but slower: $\langle V_c \rangle \sim 100$ km/s)



A slight asymmetry of the bulge and additional kinematic data show that the Milky Way has a central bar extending to $R=2-3$ kpc. It is a Sbc galaxy or SABbc(r) - there can be no perfect agreement when looking at multi-wavelength data!

The center of the Galaxy (nucleus) is a very exotic place, with the Sagittarius A* radio source, surrounded by a torus ($R=7$ pc) of molecular gas, which flows in at a rate of $0.001-0.01 M_{\text{sun}}/\text{yr}$ and formed dozens of massive stars within the last 3-7 Myr. Nucleus (right panel, showing gas) is much smaller than the black dot in the background picture.

A fairly dark and inactive, 'starved' black hole ($m=2-3$ mln M_{sun}) lurks in the center of Galactic Nucleus (white dot).



21 cm - line data are used to determine basic Galactic rotation

Leiden/Dwingeloo & IAR HI Surveys; $b = 0$

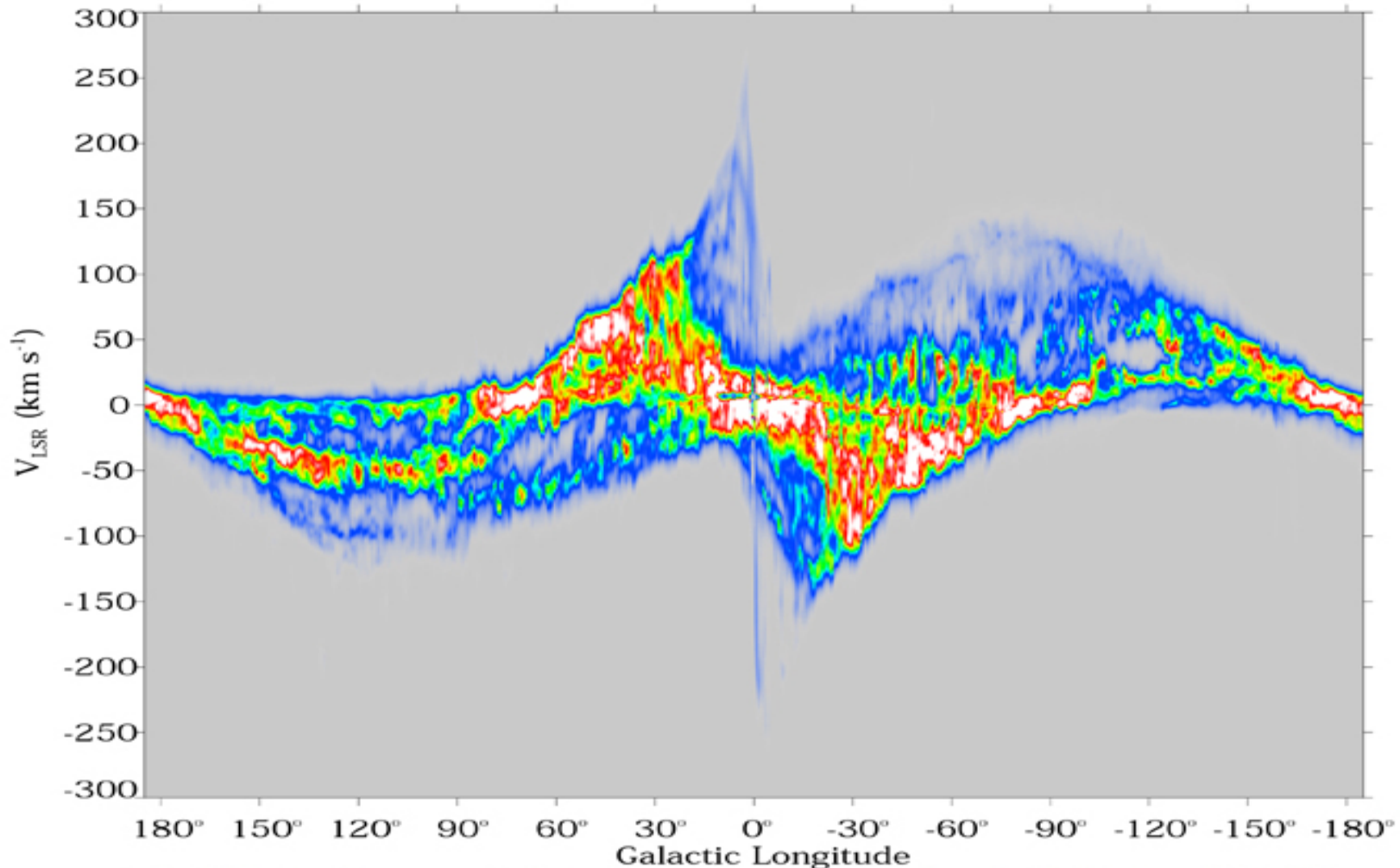


Fig 2.20 (D. Hartmann) 'Galaxies in the Universe' Sparke/Gallagher CUP 2007

Figure 2.18 In the plane of the disk, the intensity of 21 cm emission from neutral hydrogen gas moving toward or away from us with velocity V_{LSR} , measured relative to the local standard of rest – D. Hartmann, W. Burton.

Rotation curve of Milky Way is approximately flat:

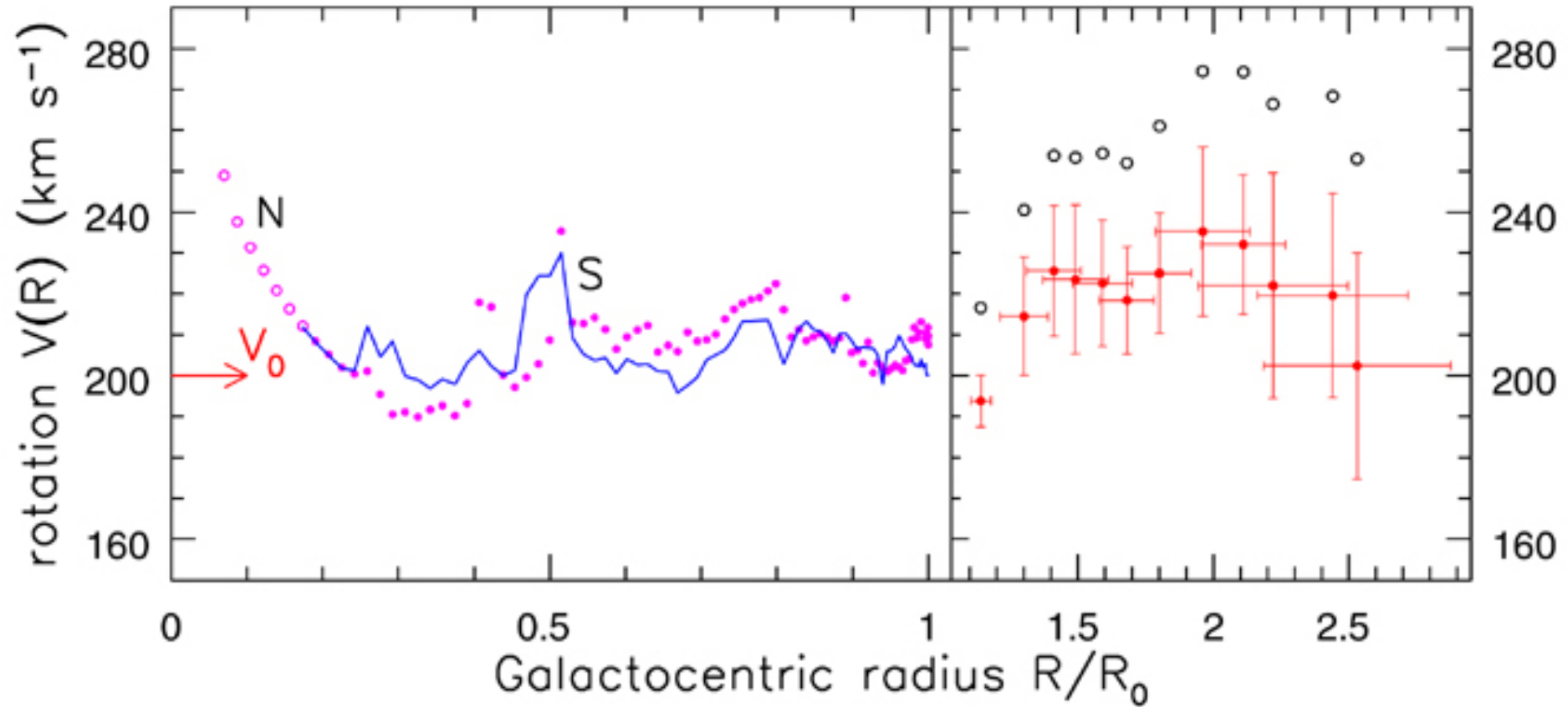


Fig 2.21 (Burton, Honma) 'Galaxies in the Universe' Sparke/Gallagher CUP 2007

ASTB23. Lecture L23

Rotation curves and spiral arms in galaxies - observations and theory

Decomposition of rotation curves

into disk, bulge, halo components

Two basic types of rotation curves.

Grand design spirals vs. flocculent spirals

Leading vs trailing spirals & how to tell one from the other

Material arms & the winding problem

Stochastic star formation

Kinematic waves: a step in the right direction

5.3.2 Dark matter in disk galaxies

We can compare the rotation curve of Figure 5.20 with what we would expect if the mass of the galaxy had been concentrated entirely in its stars and gas. For the stellar disk and the bulge, we assume that the density of stars is proportional to the R band light, and guess at the mass-to-light ratio \mathcal{M}/L . For the gas disk, the surface density is approximately 1.4 times that measured in HI, since helium contributes a mass about 40% of that in hydrogen; see Section 1.5. We calculate the contributions to the radial force from each component separately, and we add them to find the total. Thus $V^2(R)$ for the galaxy is the sum of contributions from the various parts.

(superposition principle for gravitation)

Taking the bulge to be nearly spherical, we can find its inward force from Equation 3.20. Because the stellar and gas disks are flattened, their force can point either inward or outward. At $R \lesssim 6$ kpc, the force from the gas disk is outward, making a negative contribution to $V^2(R)$. In Figure 5.20, the ratio \mathcal{M}/L has been adjusted so that gas and luminous stars account for as much of the galaxy's rotation as possible: this is the 'maximum disk' model. If no other matter had been present, we see from Figure 5.20 that the rotation speed should have begun to fall at around 20 kpc from the center. Like the Milky Way, this galaxy contains substantial mass in regions beyond the visible stellar disk. The curve labelled 'halo' shows how a spherical halo of dark matter could provide enough inward force to account for the measured rotation speed; at least 75% of the total mass appears to be dark. The outer reaches of this galaxy contain almost exclusively HI gas and unseen matter.

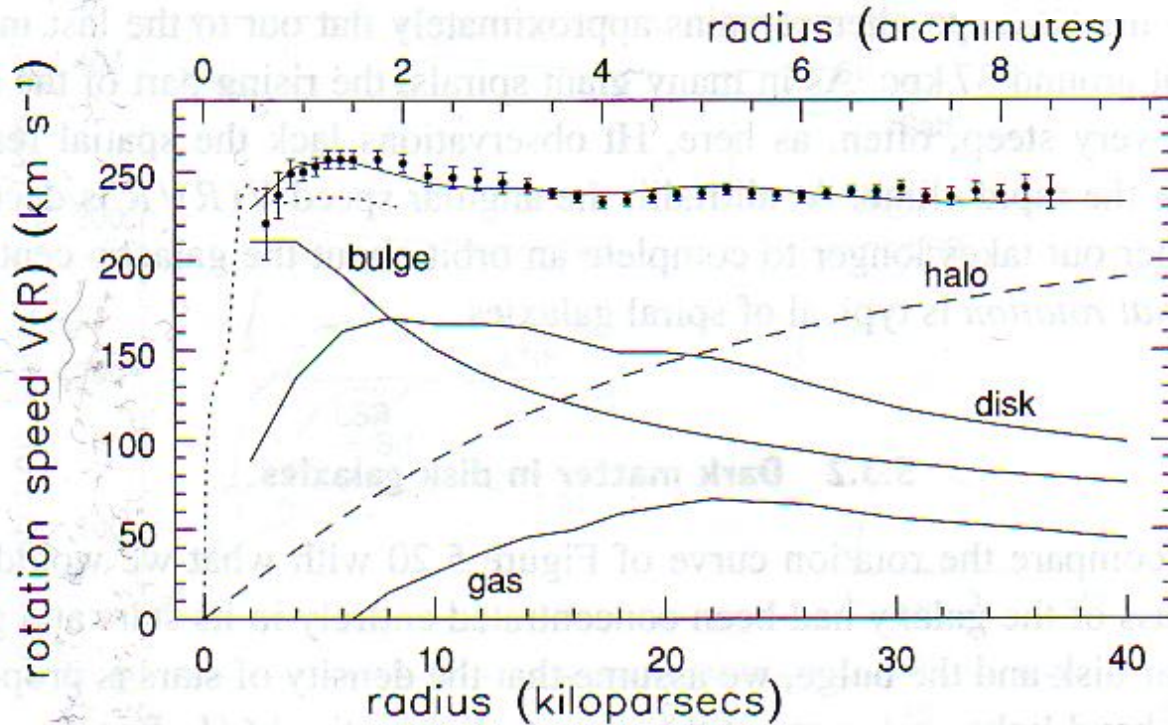
(next slide)

Decomposition of the rotation curve of NGC 7331- a Milky Way-like galaxy



Decomposition of the rotation curve of NGC 7331 giving the best fit to the observations

$$\frac{V^2(R)}{R} = \frac{GM(<R)}{R^2}$$



If there are several subsystems (e.g. gas, stars in a disk, halo) contributing to $M(<R)$, then the rotation curve is a sum of **squares** of several rotation curves.

Figure 5.20 Points give rotation curve of NGC 7331, as found from the HI map of Figure 5.13; vertical bars show uncertainty. CO gas (dotted), observed with a finer spatial resolution, traces a faster rise. The lower solid curves show contributions to $V(R)$ from the gas disk, the bulge, and the stellar disk. A dark halo (dashes) must be added before the combined rotation speed (uppermost curve) matches the measured velocities – K. Begeman, Y. Sofue.

A spherically-symmetric dark **halo** density-velocity model often used for spiral galaxies

$$\rho_h = \rho_h^0 \left[1 + \frac{R^2}{R_{\text{core}}^2} \right]^{-1},$$

$$v_h = v_h^{\text{max}} \sqrt{1 - \frac{R_{\text{core}}}{R} \arctan\left(\frac{R}{R_{\text{core}}}\right)},$$

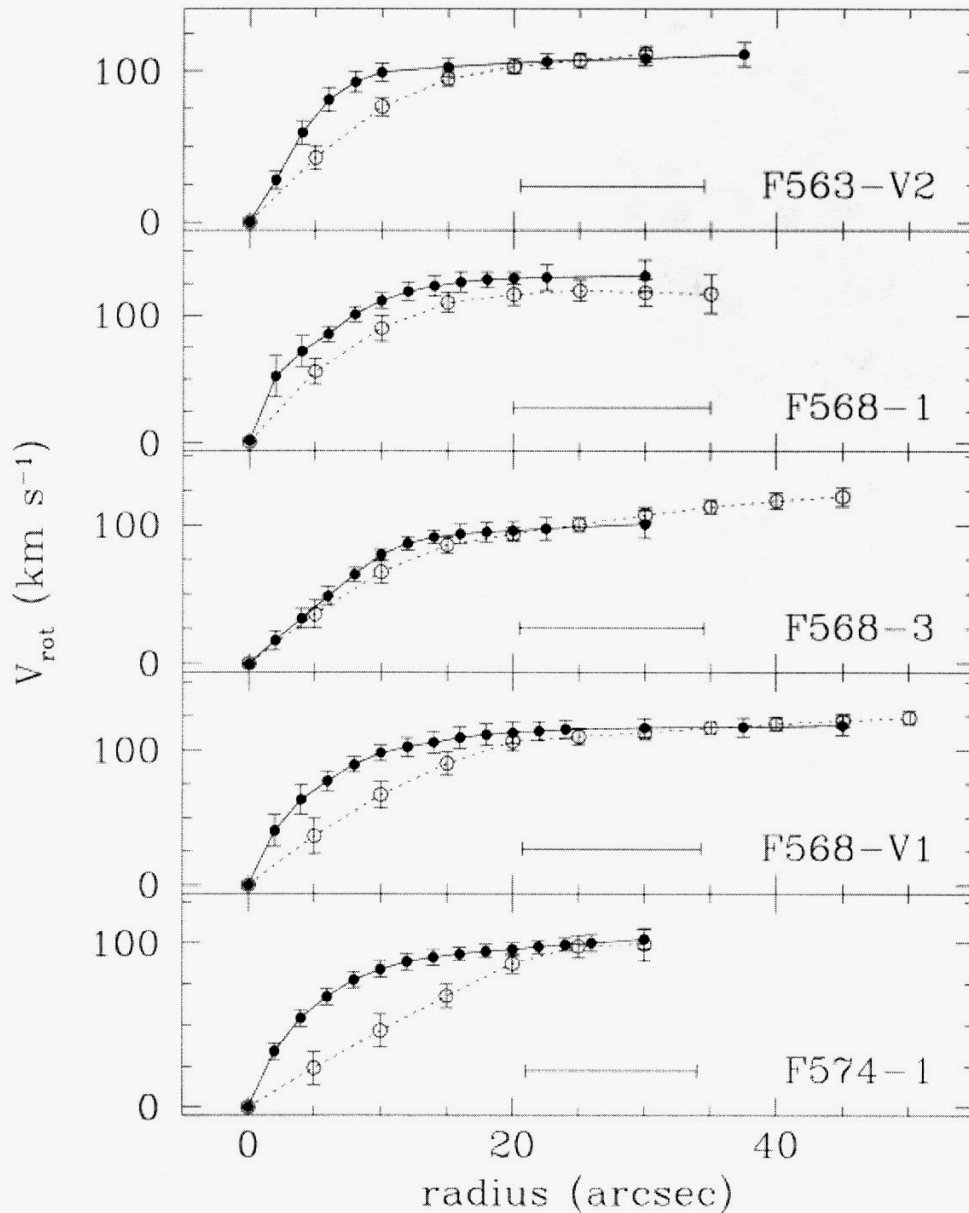
$$v_h^{\text{max}} = \sqrt{4\pi G \rho_h^0 R_{\text{core}}^2}.$$

total rotation curve contributions sum up quadratically:

$$V_{\text{total}}^2 = V_{\text{stars}}^2 + V_{\text{gas}}^2 + V_{\text{halo}}^2$$

PLOT 11.

The high-resolution $H\alpha$ rotation curves (*filled circles, solid lines*) and the H I rotation curves from BM (*open circles, dotted lines*). The horizontal bar shows the FWHM beam size of the H I observations.



The previous example is typical – most galaxies have rotation curves that do not fall toward zero at the largest observed radii

Peak rotation speeds in spiral galaxies are usually $150\text{--}300\text{ km s}^{-1}$. They rarely rise above 400 km s^{-1} , and the fastest measured rotation is about 500 km s^{-1} , in the S0/Sa galaxy UGC 12591. Larger galaxies, with longer scale lengths h_R , generally rotate more rapidly; these tend to be the Sa and Sb galaxies, rather than the Sc, Sd, and Sm systems. The rotation curves of Sa and Sb galaxies initially climb steeply, showing that relatively more of their mass is closer to the center. In these systems, the luminous matter in the disk and the bulge is concentrated at small radii, and the dark matter in the halo also becomes very dense there.

In Sd and Sm galaxies, the rotation speed increases more gradually. These galaxies do not have large bulges, and Figure 5.8 showed us that their luminous disks have low central surface brightness. The rotation curves show that the dark halo also lacks central concentration; its core, where the density is nearly constant, must be larger in relation to the galaxy's stellar disk. Most low-surface-brightness galaxies rotate slowly, with gently ascending rotation curves like those of Sd or Sm galaxies; but there are some with higher speeds, and faster-rising rotation curves.

The proportion of dark matter required to explain these rotation curves varies from about 50% in Sa and Sb galaxies to 80–90% in Sd and Sm galaxies. There may be yet more dark material out beyond the last point where we have observed HI

Asymptotic velocity

Gradual rise of rotation curve: a sign of large core of DM halo

Dark matter (DM) contents

Notice how the three aspects of dark matter vary with galaxy type

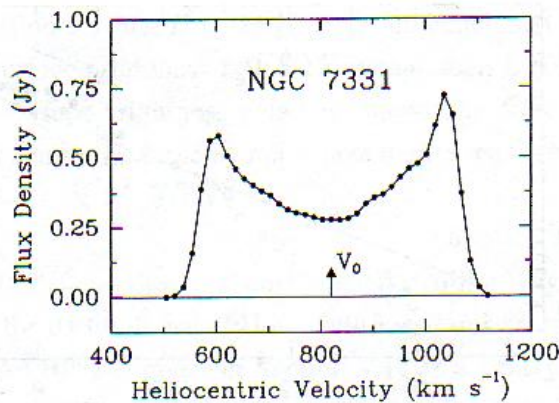


Figure 5.22 The HI global profile for NGC 7331: radio power F_ν (in janskys) received from gas moving at each velocity, measured with respect to the Sun; $V_0 = V_{\text{sys}}$, the recession speed at the galaxy center – K. Begeman.

Tully-Fisher relationship,
a correlation
between the luminosity
and maximum
rotation speed
of disk galaxies

Brighter galaxies rotate faster on average, which tells us that they are more massive. Brent Tully and J. Richard Fisher showed that the rotation speed of a galaxy increases with its luminosity, roughly as $L \propto V_{\text{max}}^\alpha$, with $\alpha \sim 4$: this is the *Tully-Fisher relation*. The observed values fall closer to a single curve when L is measured in the red or near-infrared. The blue luminosity is more likely to fluctuate over time, since young massive stars contribute much of the light. In the blue, a galaxy that has recently had a burst of star formation will temporarily be much brighter than it usually is, while V_{max} remains unchanged; so the observed luminosities will scatter widely about their mean at any given rotation speed.

Figure 5.23 plots the width of the global profile against the apparent magnitude measured at $K' \approx 2.2 \mu\text{m}$ for galaxies in the Ursa Major group; the luminosity increases slightly slower than the fourth power of V_{max} . Another recent study, measuring the galaxy light in the H band at $1.65 \mu\text{m}$, found

$$\frac{L_H}{3 \times 10^{10} L_{H,\odot}} \approx \left(\frac{V_{\text{max}}}{196 \text{ km s}^{-1}} \right)^{3.8} \quad (5.5)$$

Tully-Fisher

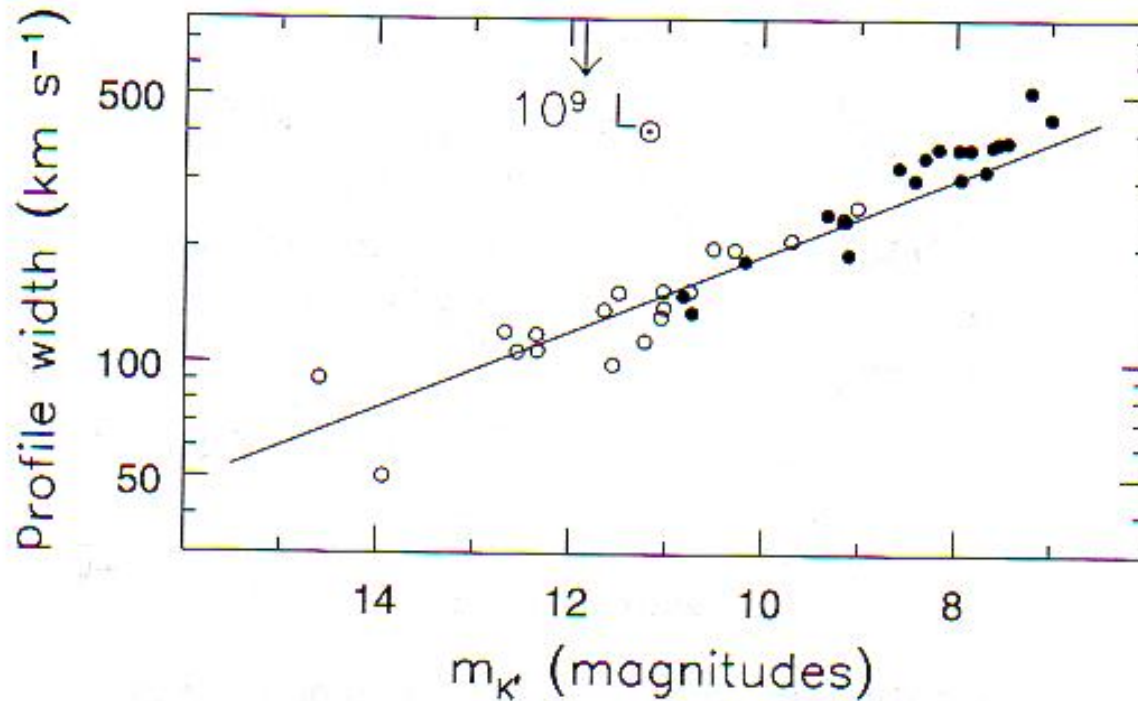
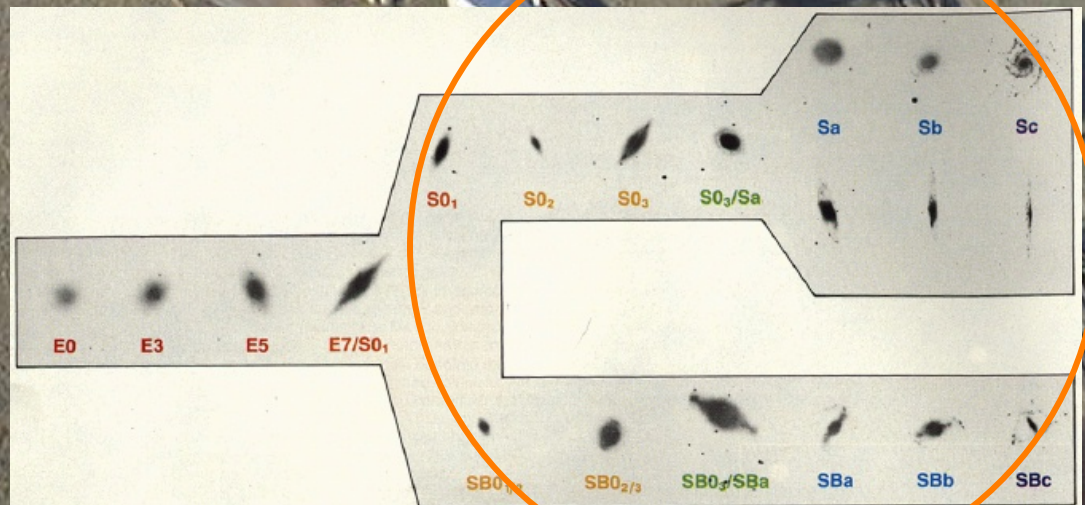
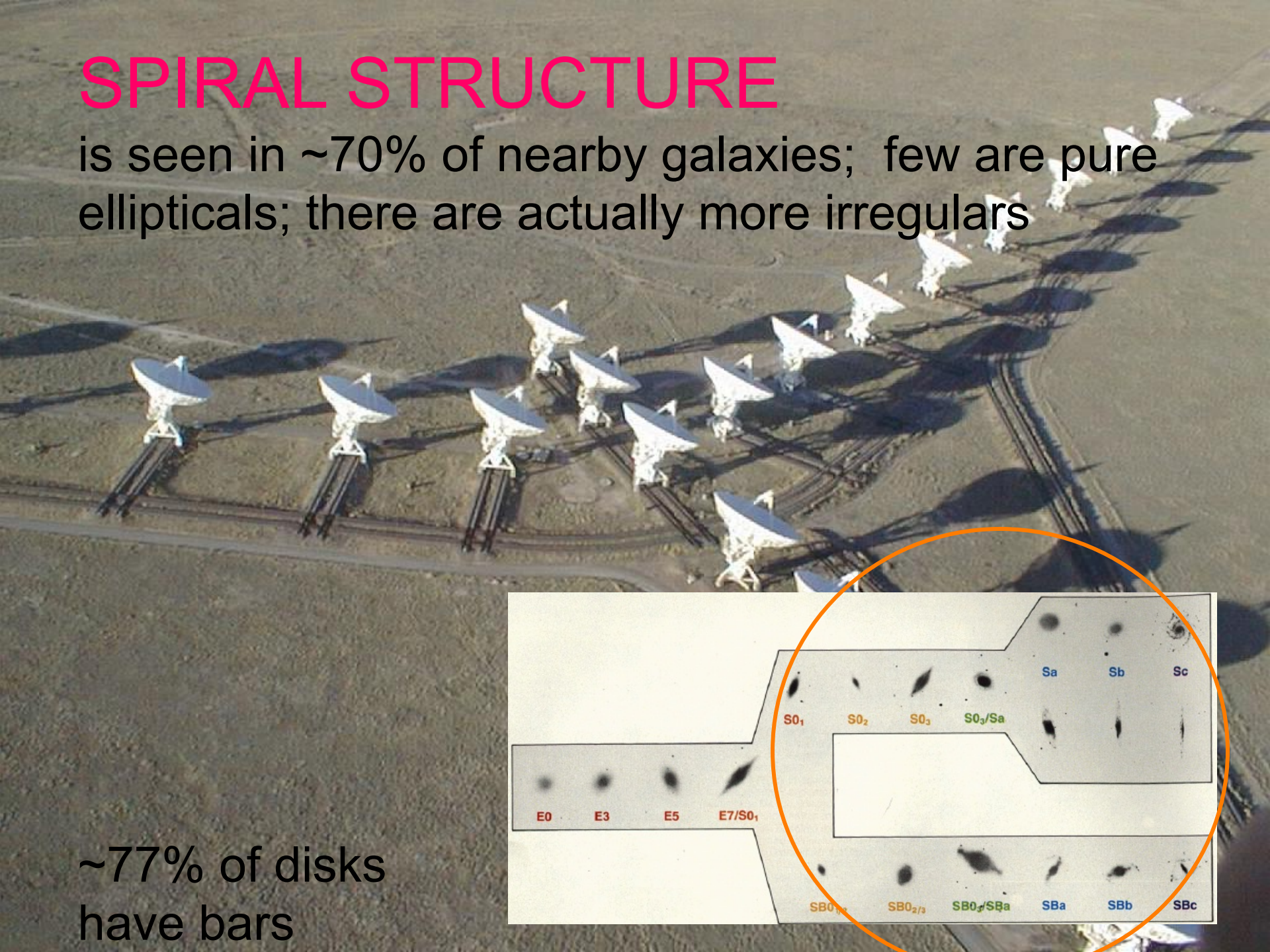


Figure 5.23 For galaxies in the Ursa Major group: from the HI global profile, width $W/\sin i \approx 2V_{\max}$ plotted against apparent K' -magnitude. Low-surface-brightness galaxies (open circles) follow the same relationship as those of high surface brightness (filled circles). The solid line passing through $L = 3 \times 10^{10} L_{\odot}$, $V_{\max} = 205 \text{ km s}^{-1}$ has slope $L \propto V_{\max}^4 - M$. Verheijen.

SPIRAL STRUCTURE

is seen in ~70% of nearby galaxies; few are pure ellipticals; there are actually more irregulars



~77% of disks
have bars

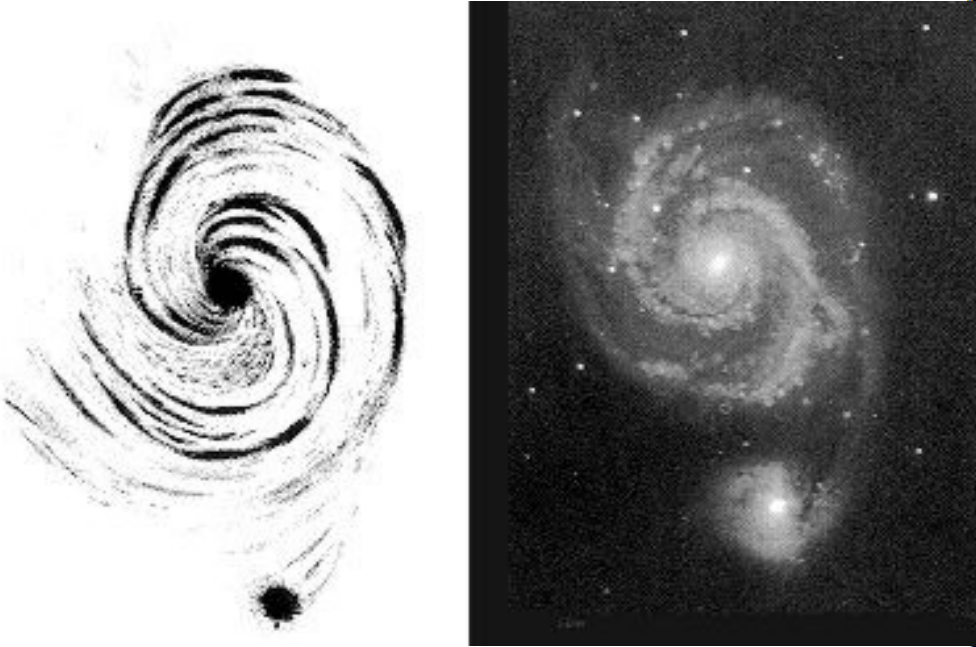


M 74

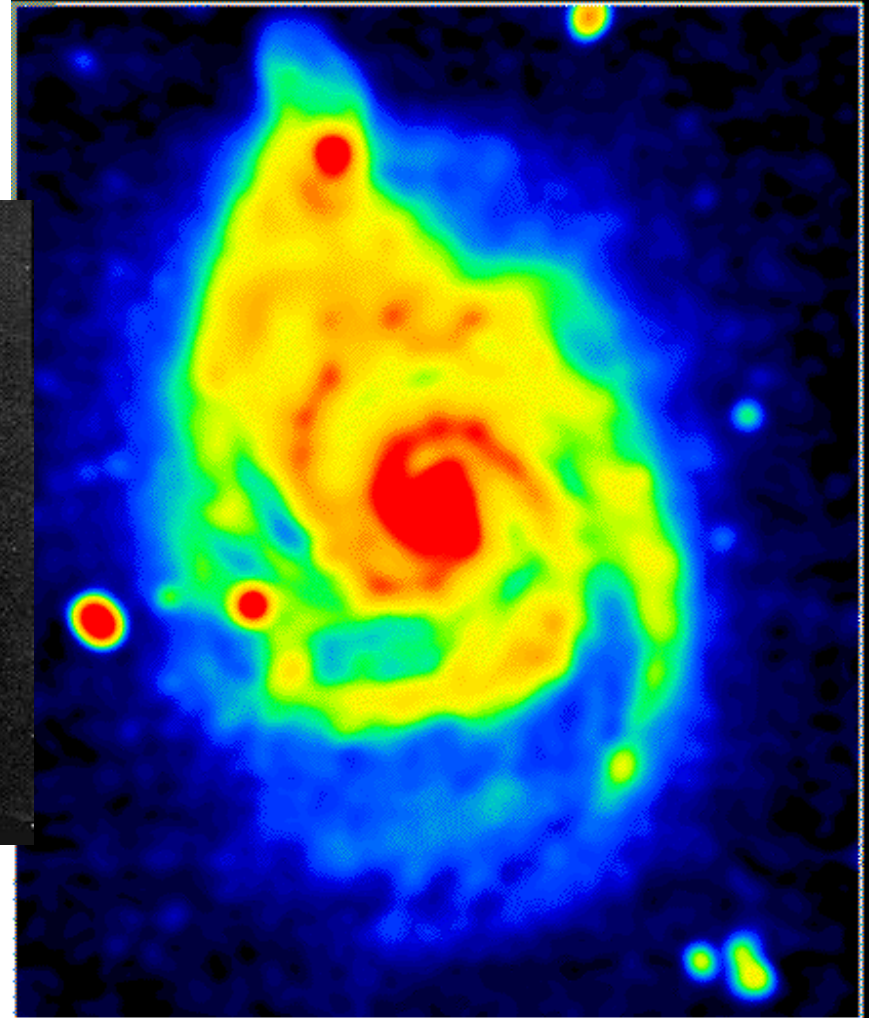
A grand-design spiral: M51

A typical radio-map of HI at 20cm

Optical image, for comparison:
(not to scale)

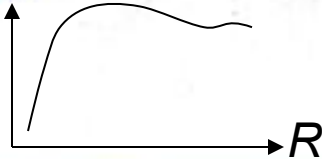


M51 20cm Total Intensity (VLA)



Notice two different types of rotation curves

Table 5.1 The sequence of luminous disk galaxies

Characteristic	<i>SO–Sa</i>	<i>Sb–Sc</i>	<i>Sd–Sm</i>
Spiral arms	absent or tight		open spiral
Color	red: late G star	early G star	blue: late F star
$B - V$	0.7–0.9	0.6–0.9	0.4–0.8
$1550 \text{ \AA} - V$	4 to 2	2 to 0	0 to -1
Young stars	few		relatively many
HII regions	few, small		more, brighter
Gas	little gas		much gas
$\mathcal{M}(HI)/L_B$	$\lesssim 0.05$ to 0.1		~ 0.25 to >1
L_B	luminous		less luminous
$I(0)$	$(1-4) \times 10^{10} L_{\odot}$		$(<0.1-2) \times 10^{10} L_{\odot}$
	high central brightness		low central brightness
	massive		less massive
$\mathcal{M}(<R)$	$(0.5-3) \times 10^{11} M_{\odot}$		$(<0.2-1) \times 10^{11} M_{\odot}$
Rotation	fast-rising $V(R)$		slowly rising $V(R)$

Note: color $1550 \text{ \AA} - V$ is defined as for $15 - V$ in Table 1.3, using flux-based magnitudes at 1550 \AA measured by OAO and ANS satellites.

About 1/3 of spiral galaxies are very regular (so-called grand design spirals)

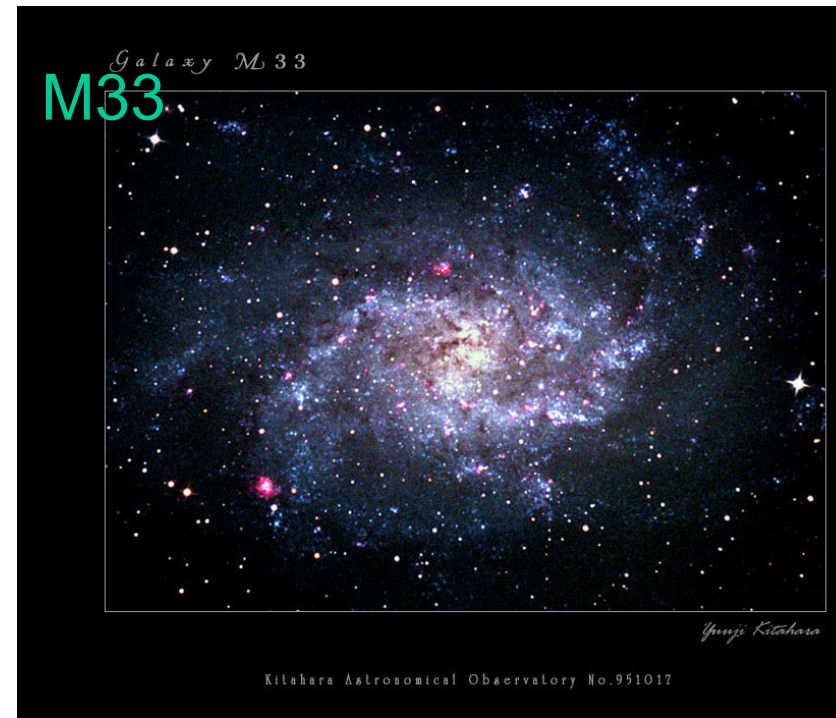


but most galaxies are flocculent, with short, torn arms

NGC 2841 (cf. Fig 5.26 in textbook)



M33



Barred Spiral Galaxy NGC 1300

Most barred galaxies show regular spirals, often attached to the bar's ends. Bars are producing those spirals, according to theory, via the so-called Lindblad resonances



Hubble
Heritage

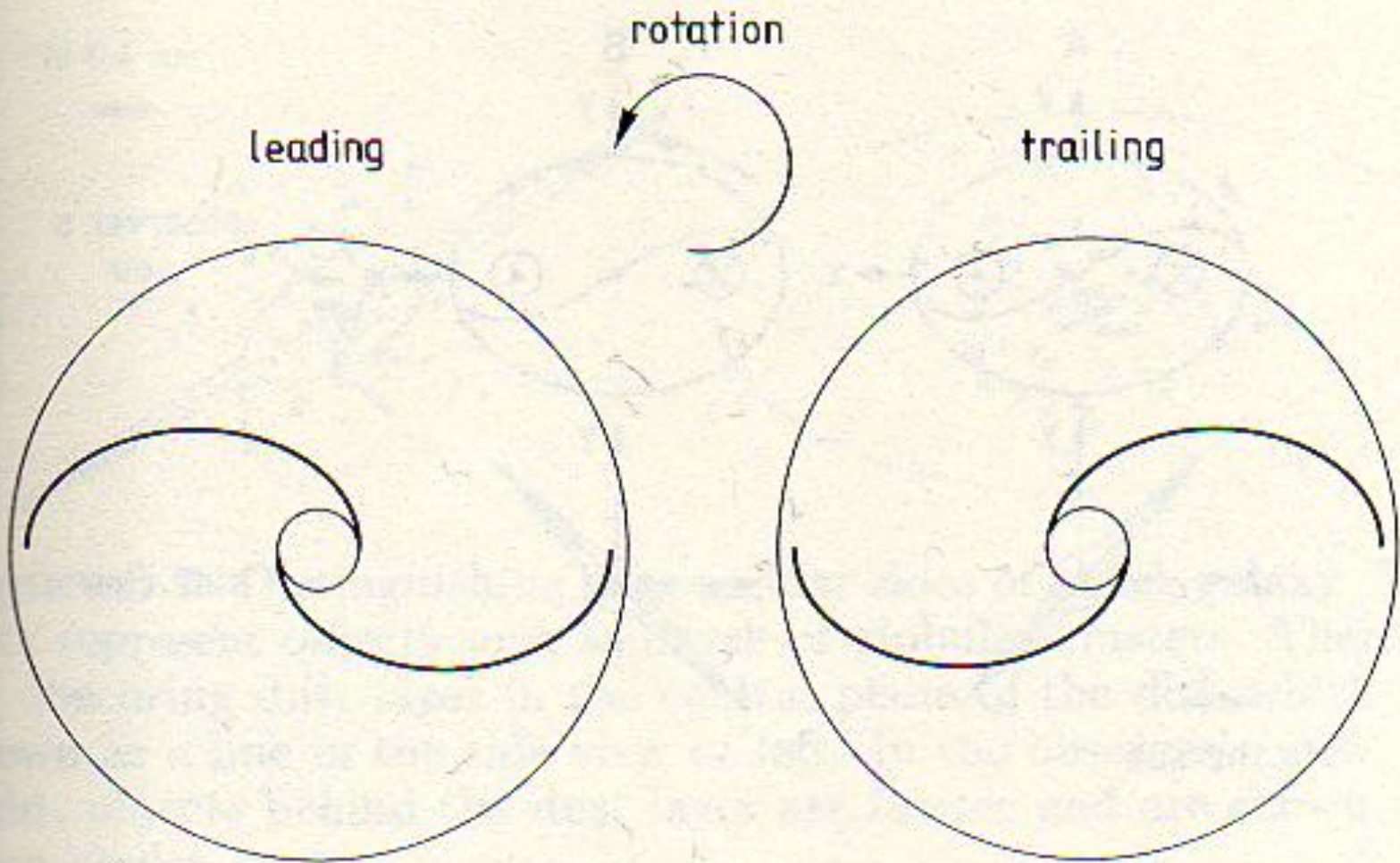
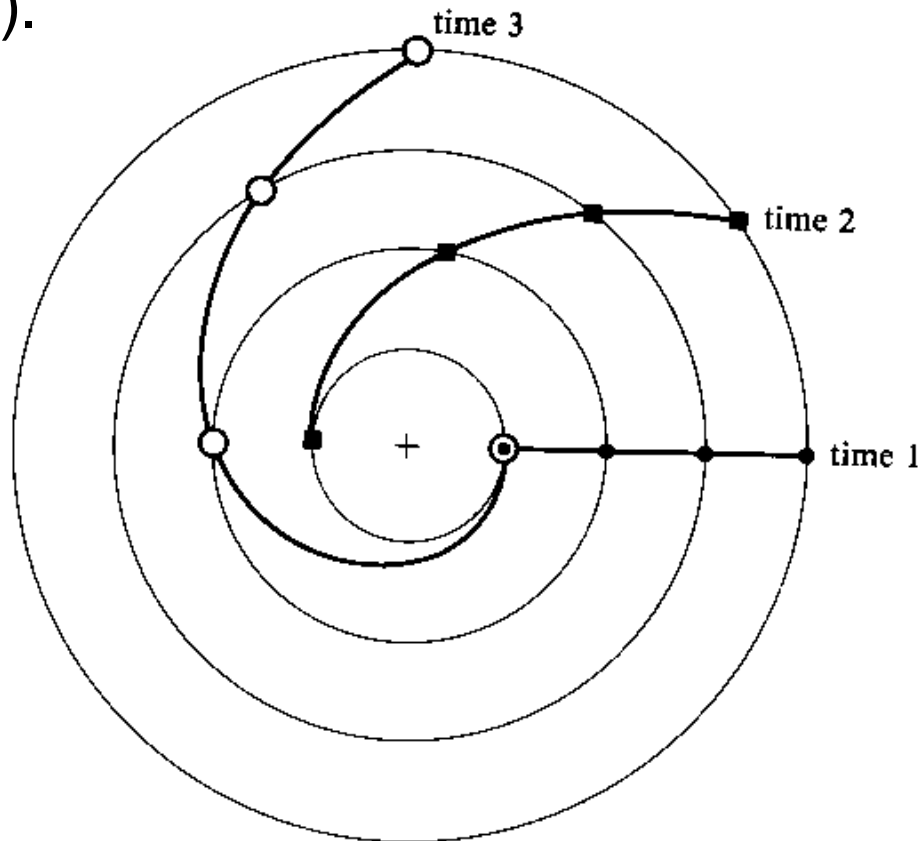


Figure 6-5. Leading and trailing arms.

One early idea was that the arms we see are **material spiral arms**, made of concentrations of stars and gas, which never leave the arms. It has the *winding problem*: if the rotation curve is flat, the angular speed is $\sim 1/R$, and the pitch angle decreases as $i \sim 1/t$ toward $i=0$ too fast, in just several galactic years (turns).



A better idea: spirals as kinematic waves forming a steady pattern

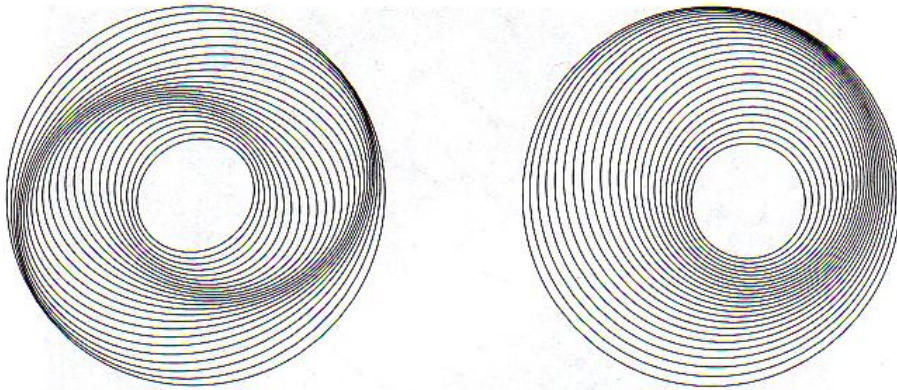
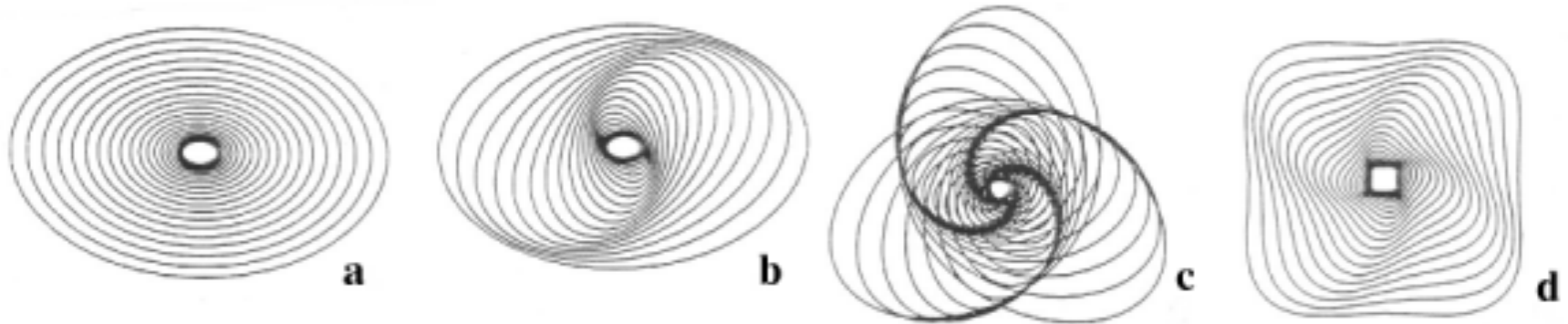
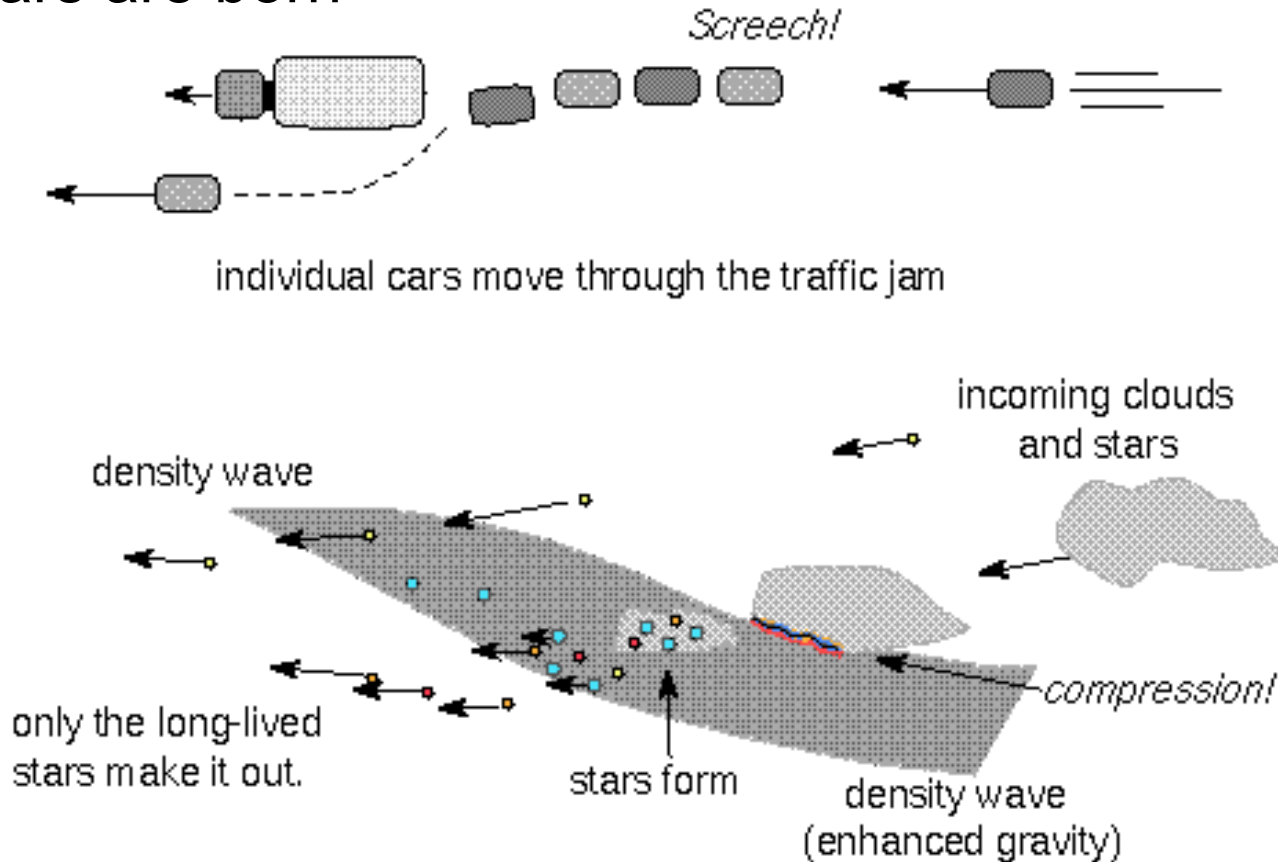


Figure 5.28 Left, oval orbits nested to form a two-armed spiral; the equation of the pattern is $R = R_g \{1 + 0.075 \cos[2(5 - 5R_g + \phi)]\}^{-1}$, and $0.3 < R_g < 1$. Right, a one-armed spiral, with $R = R_g \{1 + 0.15 \cos[(5 - 5R_g + \phi)]\}^{-1}$.

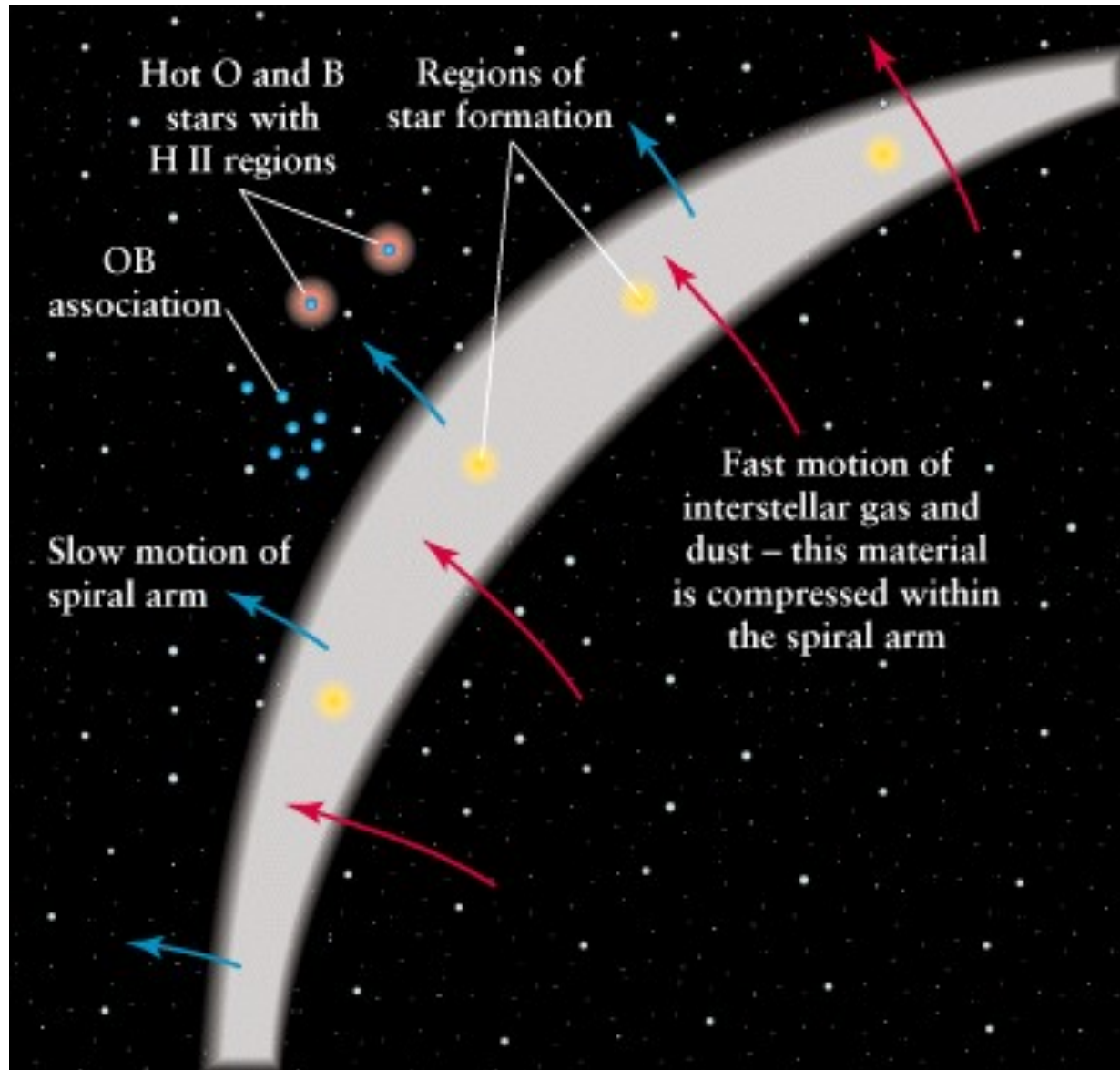
It's a nice idea but to make it work, we would need to assure that all the orbits precess (turn) at the same rate: only an additional, *dynamical* force can do this: self-gravity! This effect can only be properly calculated in a density wave theory



The best idea: spirals = density waves, or traffic jams in which new stars are born



Spiral density waves are like traffic jams. Clouds and stars speed up to the density wave (are accelerated toward it) and are tugged backward as they leave, so they accumulate in the density wave (like cars bunching up behind a slower-moving vehicle). Clouds compress and form stars in the density wave, but only the fainter stars live long enough to make it out of the wave.



Whirlpool Galaxy ■ M51



Hubble
Heritage

NASA, ESA, S. Beckwith (STScI), and The Hubble Heritage Team (STScI/AURA) • Hubble Space Telescope ACS • STScI-PRC05-12a

Finally, galactic encounters can also generate grand-designs

Spiral pattern theory

Density wave theory

The WKB dispersion relation for waves in disks

Toomre stability (gravitational stability) of disks

4 possible types of waves in galactic disks

Density wave theory of Lin & Shu

**Spiral pattern = Waves + Resonances (resonant cavity)
+ Wave amplification + Feedback**

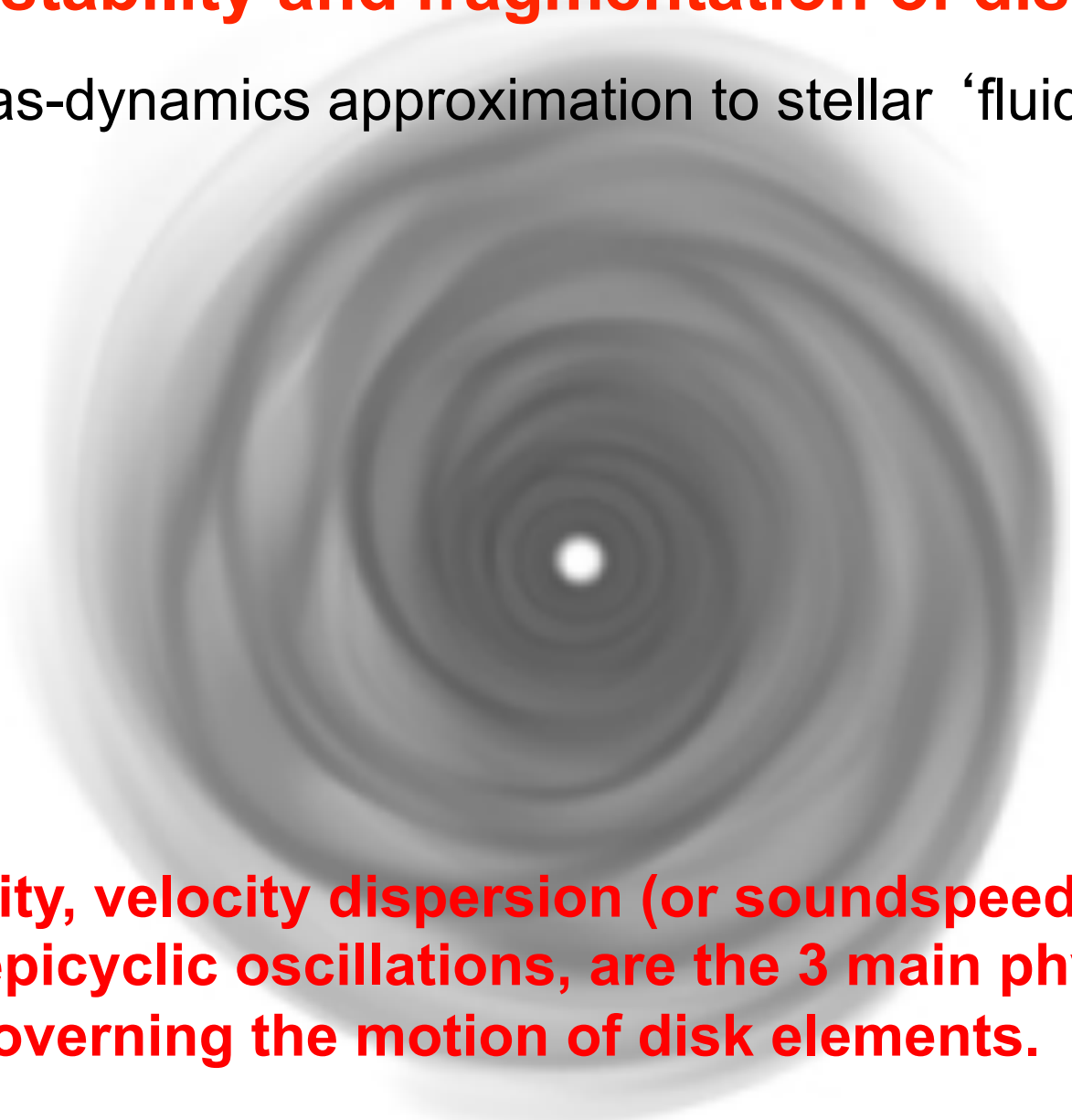
(or w/o amplification & feedback, if waves are driven by external forces like the gravity of bars or by encounters)

Growing mode cycle theories (competing!):

1. WASER amplification scheme, a slow WKB wave growth
2. SWING amplification as non-WKB rapid amplification mode

Waves, stability and fragmentation of disks

In the gas-dynamics approximation to stellar ‘fluid’



Self-gravity, velocity dispersion (or soundspeed in gas), and the epicyclic oscillations, are the 3 main physical effects governing the motion of disk elements.

$$\exp(i\psi) = \cos\psi + i\sin\psi$$

$$i = \sqrt{-1}$$

Euler formula (all the math you'll need to understand the exponential notation below). We write **complex** quantities, but remember to take a **real** part of any result in the end. It pays off...

To study waves in disks, we substitute into the equations of hydrodynamics the wave in a WKBJ (WKB) approximation, often used in quantum mechanics. Assume that waves are sinusoidal, tightly wrapped, or that $kr \gg 1$. All quantities describing the flow of gas in a disk, such as the density and velocity components (let's call them X), are given by cosines as:

$$X(r, \theta, t) \sim X_0 + X_1(r) \exp[i(m\theta + \int k dr - \omega t)] \quad (\text{observed: real part!})$$

$\omega = \omega(k) =$ *frequency of the wave inertial frame*

$k =$ *wave vector* ($k > 0$ is a trailing, $k < 0$ a leading spiral)

Some history

WKB applied to Schrödinger equation (1925)

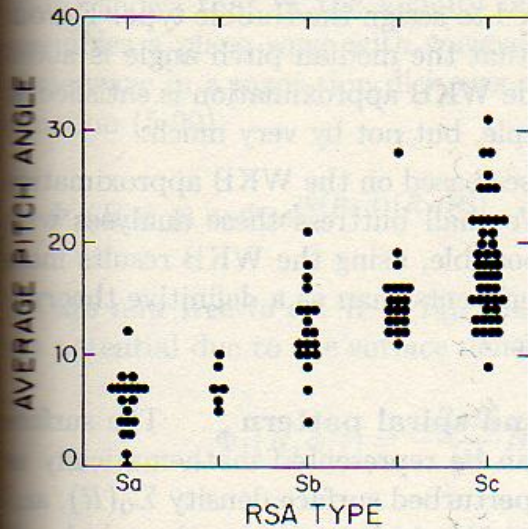
Gregor Wentzel (1898-1978) German/American physicist

Hendrick A. Kramers (1894-1952) Dutch physicist

Léon N. Brillouin (1889-1969) French physicist

Harold Jeffreys (1891-1989) English mathematician, geophysicist, and astronomer, established a general method of approximation of ODEs in 1923

} 1926



Notice the typical values of pitch angle for Sa, Sb, Sc types of: 5°, 12°, and 15°-25°, respectively

Figure 6-12. Measured pitch angle as a function of Hubble type for 113 galaxies (Kennicutt 1981). Reprinted by permission of *The Astronomical Journal*.

$|df(R, t)| = 2\pi$. If the arms are tightly wound we may replace $f(R + \Delta R, t)$ by $f(R, t) + (\partial f / \partial R)\Delta R$ so that $(\partial f / \partial R)\Delta R = 2\pi$. In this case ΔR is identical to the **radial wavelength**

$$\lambda(R, t) \equiv \frac{2\pi}{|\partial f(R, t) / \partial R|} \quad (6-10)$$

It is also useful to introduce the **radial wavenumber**

$$k(R, t) \equiv \frac{\partial f(R, t)}{\partial R} \quad (6-11)$$

Note that $\lambda = 2\pi/|k|$, but k can be positive or negative. The sign of k determines whether the arms lead or trail. If we assume that the galaxy rotates in the direction of increasing ϕ , then

$$\text{leading arms} \Leftrightarrow k < 0 \quad ; \quad \text{trailing arms} \Leftrightarrow k > 0. \quad (6-12)$$

The pitch angle i is given by equation (6-2) as

$$\cot i = \left| \frac{kR}{m} \right|. \quad (6-13)$$

$k = \frac{2\pi}{\lambda}$ (...If you ever need to find the wavelength in the radial direction, use this general formula, binding wavelength and wave number)

The wave-crest shape and angular speed Ω_p (trailing wave)

This spiral pattern has a constant shape and rotates with a constant angular speed, which we can find by taking one point $r = \text{const}$ on a wave-crest (equation on the right), and looking at how the azimuthal angle depends on time:

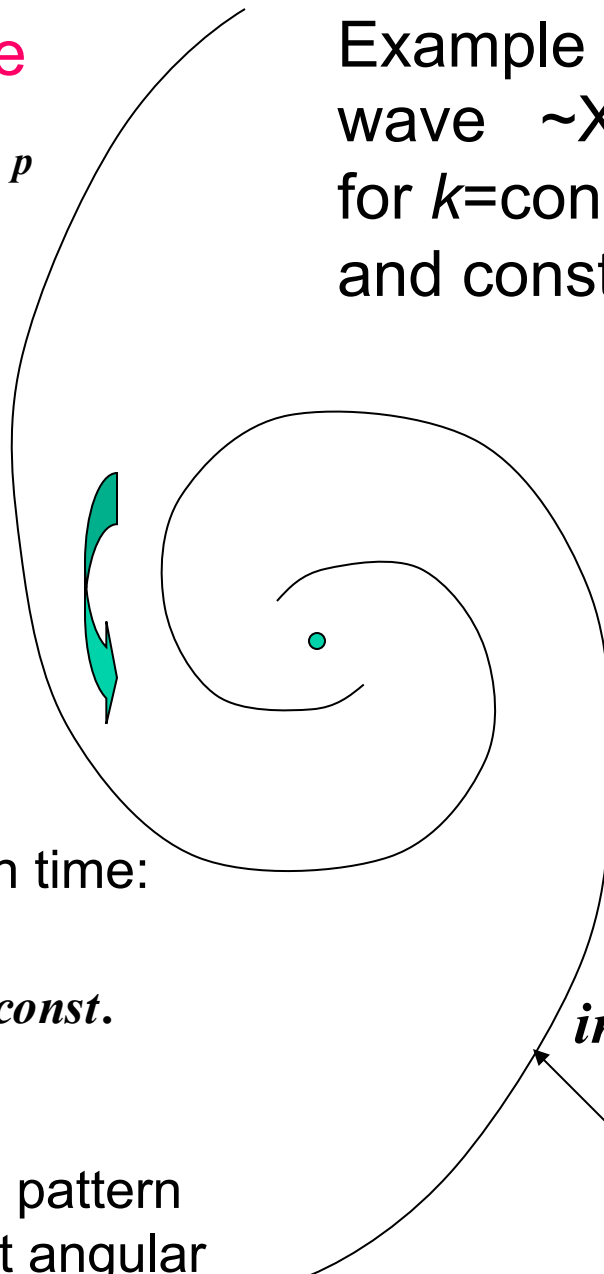
$$m\theta - \omega t = \text{const.}$$

$$\theta = (\omega/m)t + \text{const.} = \Omega_p t + \text{const.}$$

$$\Omega_p = \omega/m$$

which shows that the whole pattern rotates counter-clockwise at angular speed Ω_p

Example of a crest of the spiral wave $\sim X_1 \exp[\dots]$ for $k = \text{const} > 0$, $m = 2$, and constant time frequency ω



almost all observed patterns consist of trailing spirals

$$im\theta + i \int k dr - i\omega t = \text{const}$$

The argument of the exponential function is constant on the spiral wave-crest

A **dispersion relation** is, as in all the physics, a relation between the time and spatial frequencies, $\omega = \omega(k)$

The one describing a simple harmonic (sinusoidal) sound wave in the air:

$$\omega = \omega(k) = ck = 2\pi c / \lambda$$

$\lambda = \text{wavelength of the wave}$

(don't use that relation for galaxies, it's only good for sound or other waves travelling through uniform medium or space at speed c !)

the waves in a non-rotating medium w/o gravity are simply pure pressure (sound) waves.

The complications due to rotation lead to a spiral shape of either a sound wave, or a fully self-gravitating pressure wave.

Dispersion Relation for non-axisymmetric waves in disks *tight-winding (WKB) local approximation*

Doppler-shifted
frequency

epicyclic
frequency

self-
gravity

disk pressure
(or velocity dispersion)

$$(m\Omega - \omega)^2 = \kappa^2 - 2\pi G\Sigma |k| + c^2 k^2$$

m = number of arms (azimuthal number)

Ω = angular orbital speed

ω = frequency of the wave in the inertial frame

κ = epicyclic frequency (natural radial freq. in disk)

Σ = surface density of gas

c = soundspeed

k = wave vector (length)

e.g.,

in Keplerian disks, i.e. disks
around point-mass objects

$\kappa = \Omega =$ angular Keplerian speed

Dispersion Relation in disks with axisymmetric ($m=0$) waves

$$(m = 0) \quad \omega^2 = \kappa^2 - 2\pi G \Sigma |k| + c^2 k^2$$

$$\omega^2 \mapsto \min \Leftrightarrow \partial_k \omega^2 = 0 \Leftrightarrow |k_{cr}| = \pi G \Sigma / c^2$$

*and if we plug the above most unstable (or critical) k ,
then the smallest ω^2 is*

$$\omega^2 = \kappa^2 - (\pi G \Sigma)^2 / c^2$$

Finally, $\omega^2 \mapsto 0$ corresponds to the loss of stability

$$Q = \frac{\kappa c}{\pi G \Sigma}$$

Safronov – Toomre number

(1960 - 1964)

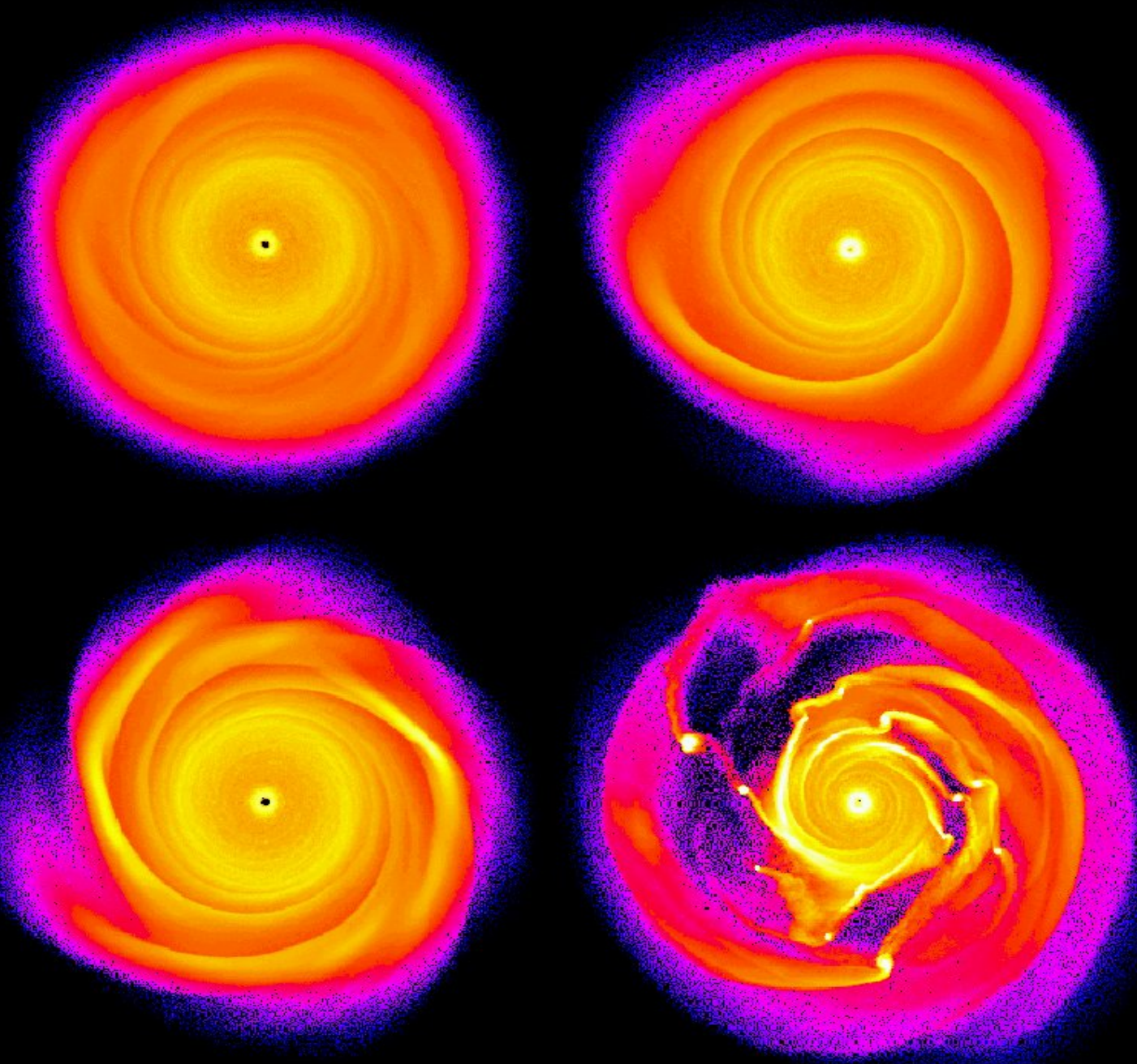
Alar Toomre (MIT)

decides about the stability : $Q < 1$ means gravit. instability

It turns out that even at $Q \sim 1.5$ there are unstable nonaxisymmetric global modes. They can be ‘grown’ numerically in an initially symmetric disk.
Observed galaxies have $Q > \sim 1.6$



Mayer, Quinn, Wadsley, Stadel (2003)



SPH =
Smoothed
Particle
Hydrodynamics

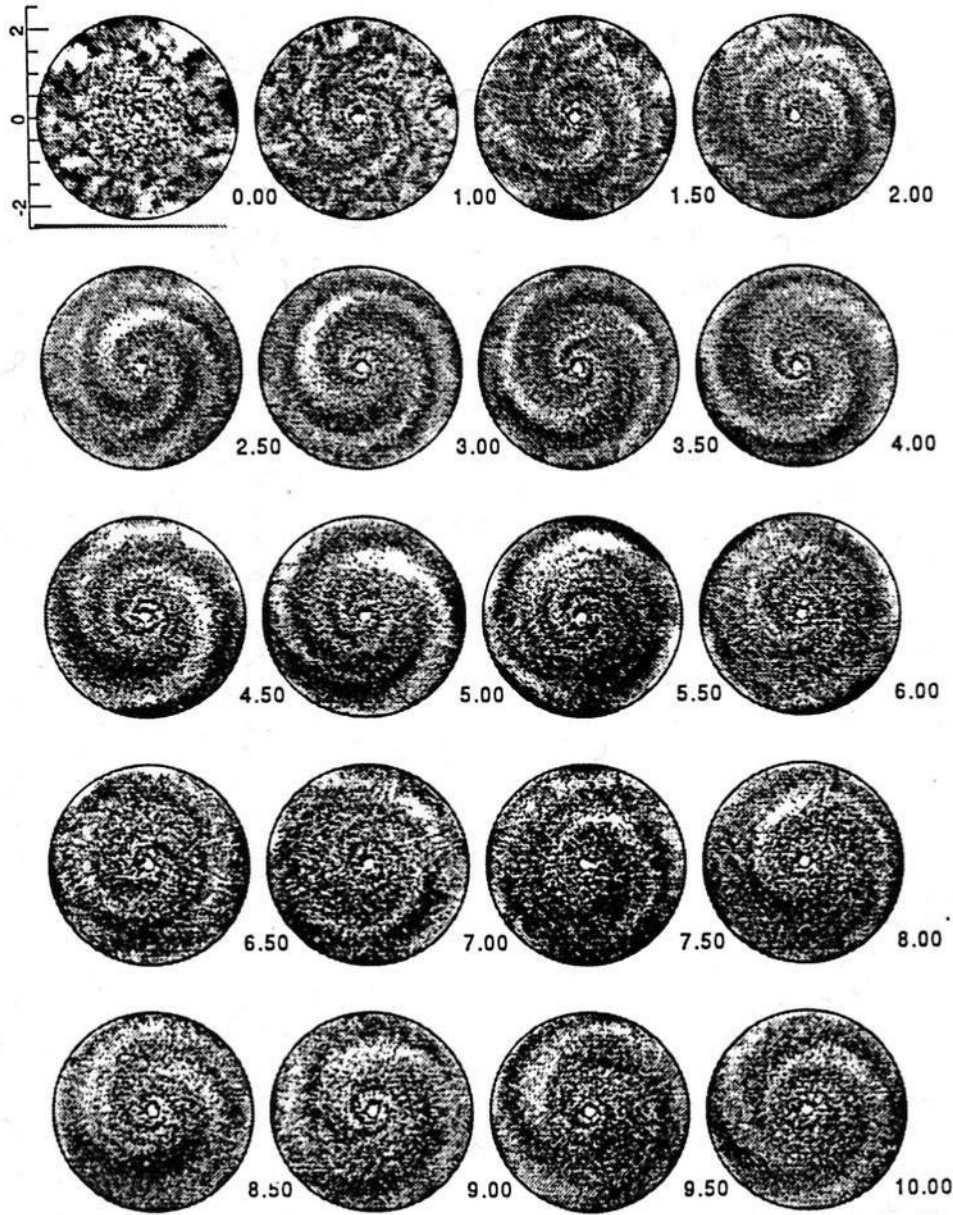
1 million particles

Isothermal disk's
gravitational
breakup

(fixed velocity
dispersion, a rather
unrealistic model of
a galaxy; stars not
gaining random
velocities from
encounters with
spiral arms.)

From: Laughlin & Bodenheimer (2001)

PROTOSTELLAR DISK EVOLUTION



Disk in this SPH (Smoothed Particle Hydrodynamics) simulation initially had $Q \sim 1.8$

The m -armed global spiral modes of the form $\exp[i(m\theta + \int k dr - \omega t)]$

grow and compete with each other. But the waves in a stable $Q \sim 2$ disk **stop growing** and do not form separate objects (baby galaxies).

The same applies to all **real disks**, which stay at $Q \sim 1.4 - 2.5$, as far as we can measure their Q factors. Close to instability, but safely stabilized by the heating effect of the huge nonlinear waves (negative feedback effect).

Dispersion Relation for non-axisymmetric waves in disks

tight-winding (WKB) local approximation

Doppler-shifted **epicyclic** **self-** **gas**
frequency **frequency** **gravity** **pressure**

$$m^2 (\Omega - \Omega_p)^2 = \kappa^2 - 2\pi G \Sigma |k| + c^2 k^2$$

This is a quadratic equation for $|k|$, the absolute value of the wave number k . It has thus up to two solutions for $|k|$ (one smaller, one larger), and hence up to four solutions for the wave-vector k :

- larger $|k|$, positive $k \implies$ **Short Trailing waves** $x < \sim \sim \sim$
- larger $|k|$, negative $k \implies$ Short Leading waves $x \sim \sim \sim >$
- smaller $|k|$, positive $k \implies$ Long Trailing waves $x \sim \sim \sim >$
- smaller $|k|$, negative $k \implies$ Long Leading waves $x < \sim \sim \sim$

The first type of waves are the ones we see as *the* spiral pattern in galaxies. They travel inward toward the galactic center (x)

Other waves travel in the indicated directions. Outward-going waves are also important, they provide the feedback for the amplification cycle of waves.

Modal theory of density waves in galaxies (Lin-Shu theory)

Quasi-stationary Spiral Structure hypothesis of C.C. Lin

and F. Shu (1964)

1. Pattern rotates at constant speed:

it is a growing mode of oscillations

2. Waves are of 4 types (S.T., S.L., L.T., L.L.)

3. They propagate in a part of the galaxy

bordered by resonances and/or turning-points which deflect (refract) waves in a differentially rotating disk.

4. That part acts as a resonant cavity for waves

5. Waves are growing in the stellar disk, but do not reach large amplitude (arm vs. interarm density contrast) before saturating (levelling off).

6. Saturation is due to the transfer of wave energy to gas disk

7. Gas disk is colder kinematically and responds much more vigorously to the gravitational forces of the spiral wave in a stellar disk than that disk itself. As a consequence, gas waves steepen into shock waves:

the non-linear, easily visible density waves that we see.

8. Waves grow between the Inner Lindblad Resonance and Corotational Res.

9. Waves can propagate beyond Corotation to Outer LR. LR's kill waves.

10. CR region acts as an amplifier of waves due to over-reflection (see below)

Frank Shu

(UC Berkeley,
UC San Diego)

a well-know
astro-dynamicist





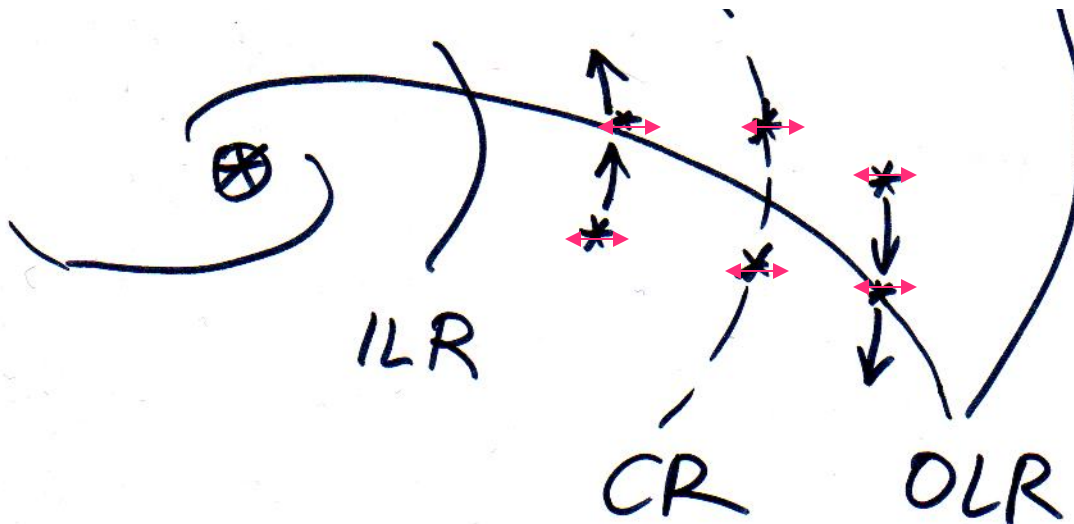
Lindblad Resonance (LR)

$$m(\Omega - \Omega_p) = \pm \kappa$$

Swedish theorist who proposed an early version of the density wave theory

The left-hand side is the frequency with which disk material (stars) encounters arms. Sometimes called the Doppler-shifted driving frequency

↑
epicyclic
freq.

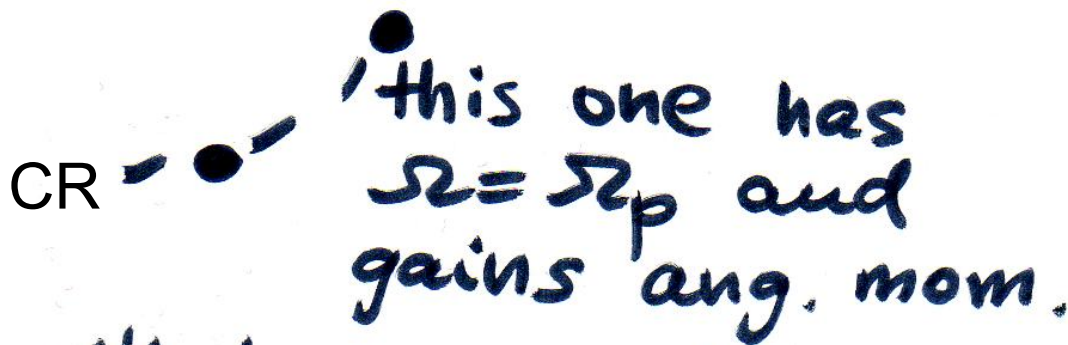
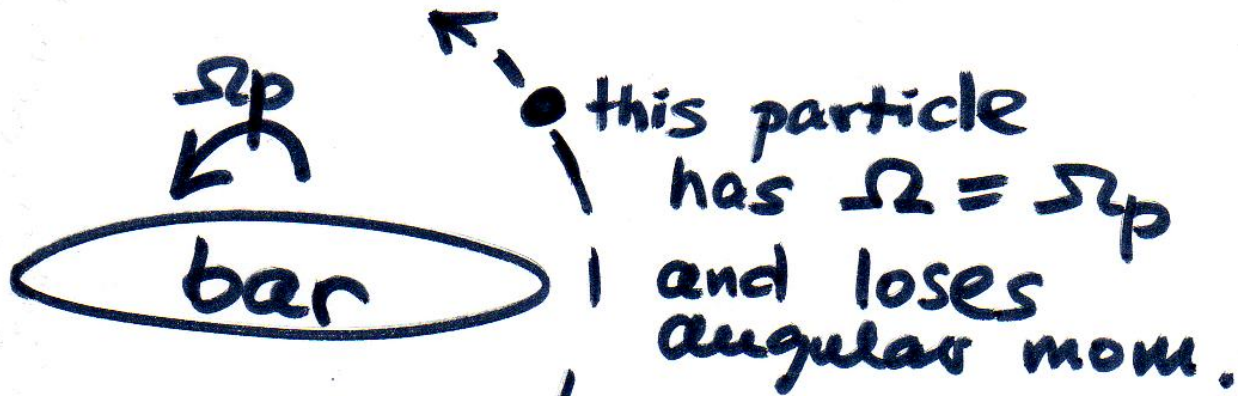


ILR = Inner LR
OLR = Outer LR

Schematic stellar motion w.r.t. spiral arm

COROTATIONAL RESONANCE (CR)

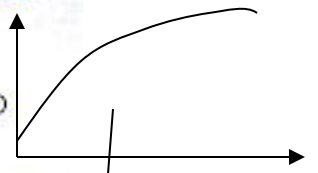
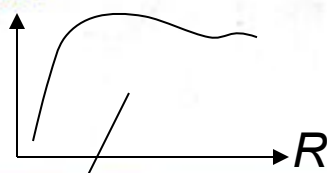
$$\Omega = \Omega_p$$



Both will be removed secularly from their orbits

Table 5.1 The sequence of luminous disk galaxies

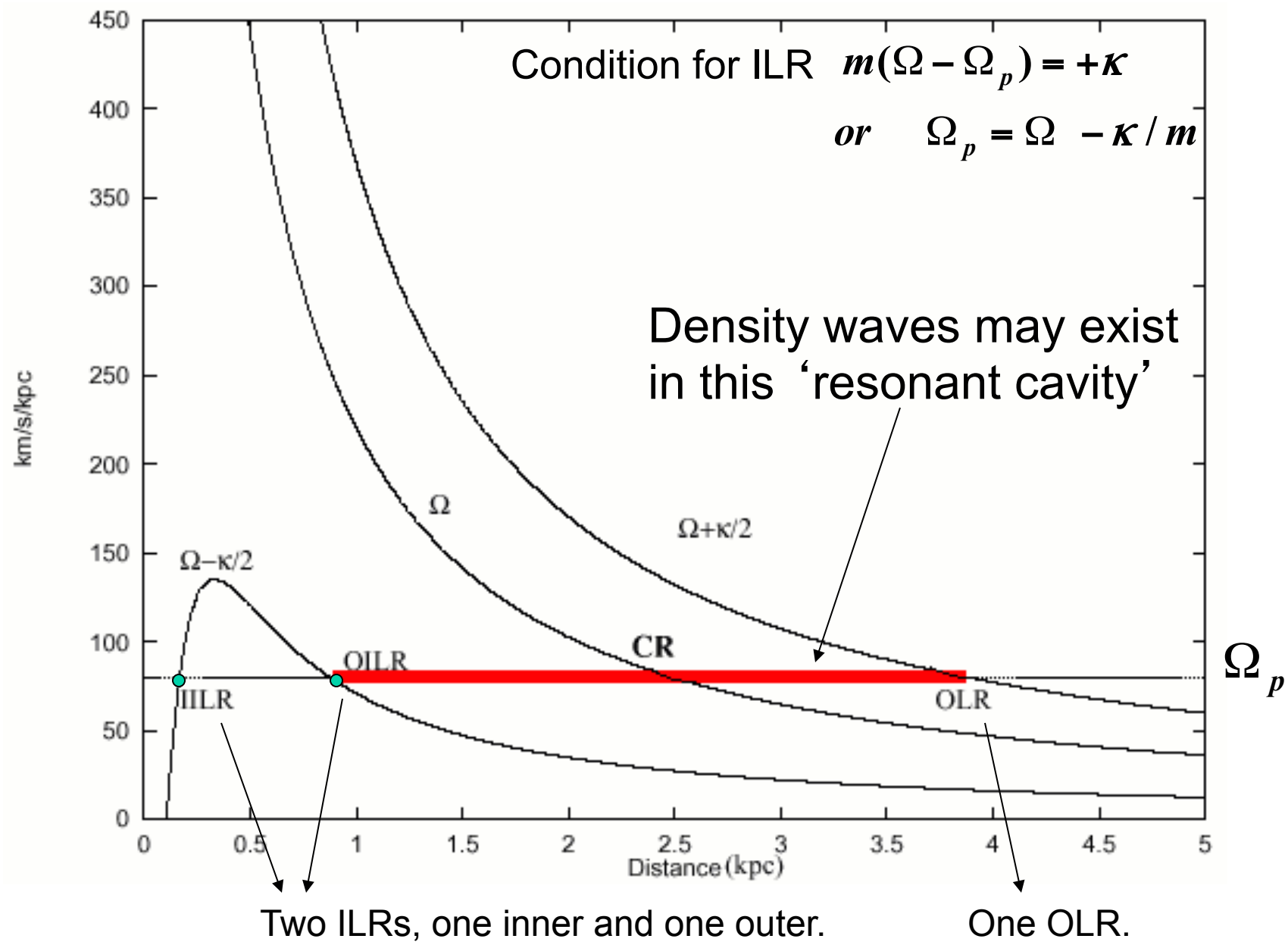
Characteristic	<i>S0–Sa</i>	<i>Sb–Sc</i>	<i>Sd–Sm</i>
Spiral arms	absent or tight		open spiral
Color	red: late G star	early G star	blue: late F star
$B - V$	0.7–0.9	0.6–0.9	0.4–0.8
$1550 \text{ \AA} - V$	4 to 2	2 to 0	0 to -1
Young stars	few		relatively many
HII regions	few, small		more, brighter
Gas	little gas		much gas
$\mathcal{M}(HI)/L_B$	$\lesssim 0.05$ to 0.1		~ 0.25 to > 1
L_B	luminous		less luminous
$I(0)$	$(1-4) \times 10^{10} L_\odot$		$(< 0.1-2) \times 10^{10} L_\odot$
$\mathcal{M}(<R)$	high central brightness		low central brightness
Rotation	massive		less massive
	$(0.5-3) \times 10^{11} M_\odot$		$(< 0.2-1) \times 10^{11} M_\odot$
	fast-rising $V(R)$		slowly rising $V(R)$



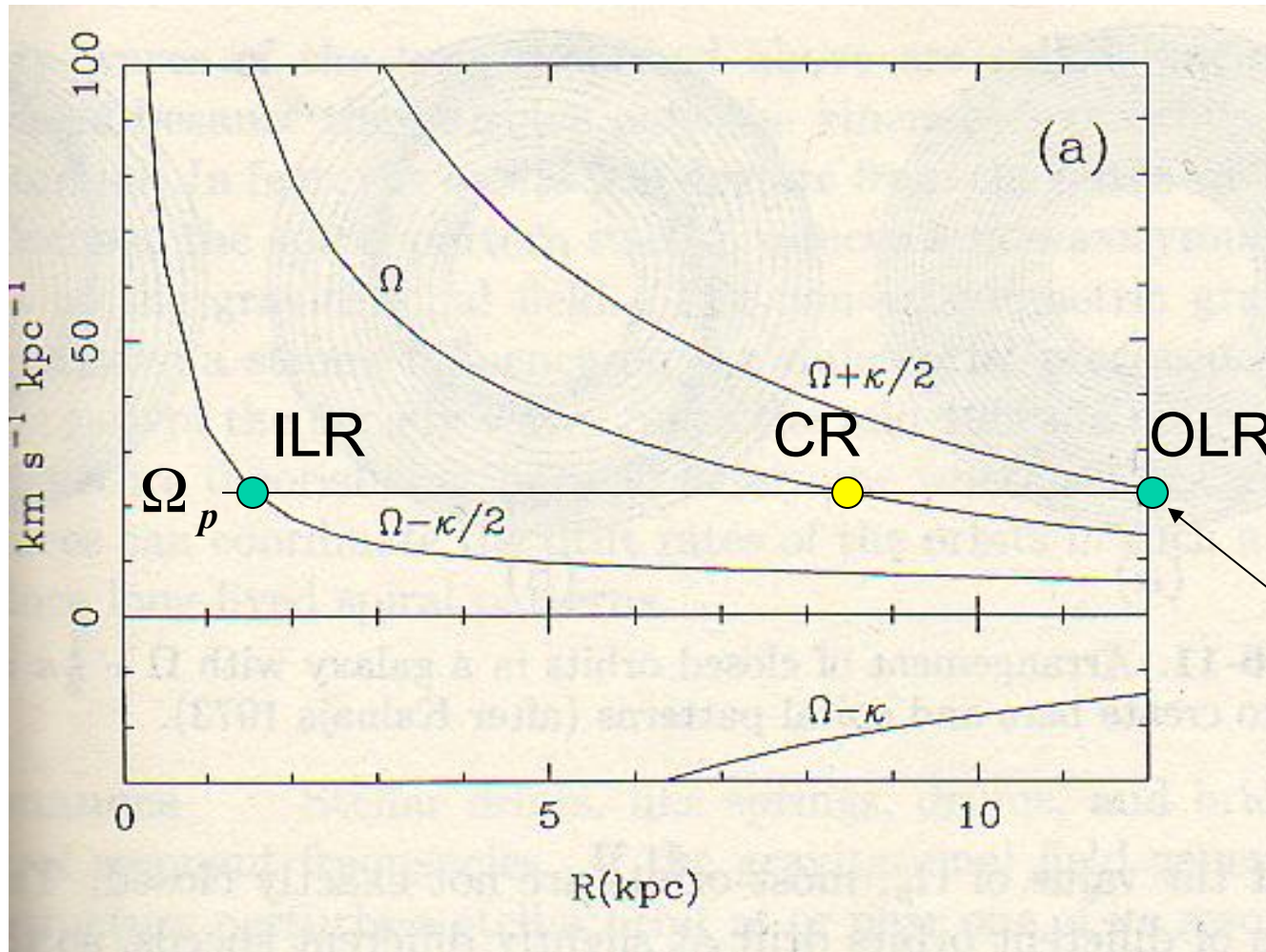
Typically one (or two) ILRs

typically no ILR

Situation typical for a rapidly rising rotation curves with a bend/knee (like in a Plummer potential): there is one or two inner Lindblad resonances



Just **one** ILR in a Soneira-Bahcall model of Milky Way

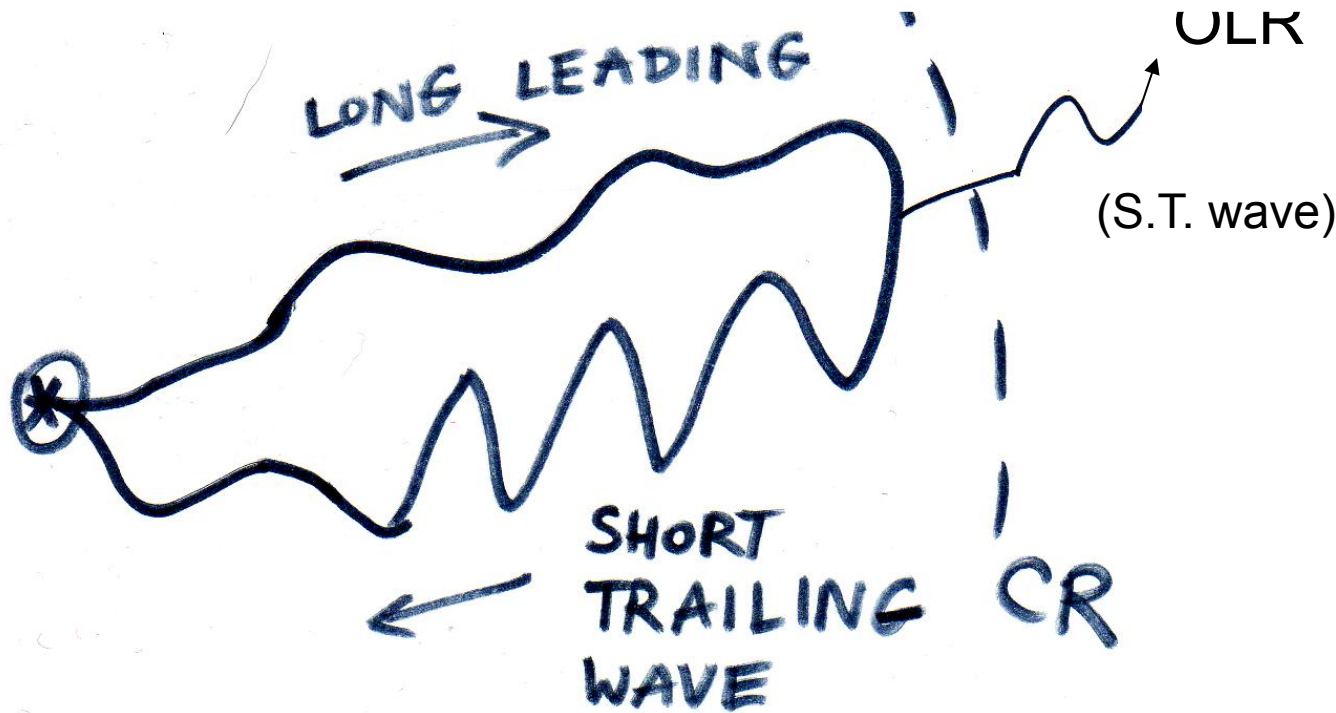


OLR condition:
 $m(\Omega - \Omega_p) = -\kappa$
 or $\Omega_p = \Omega + \kappa/m$

Similar pictures drawn for the $m=3, 4, 5, \dots$ wave pattern generate much smaller radial ranges supporting these patterns (compared with 1.5-12 kpc for $m=2$ in this example).

That explains why **real galaxies select $m=2$ as their favorite mode**. Creation of a mode (any m) is an energetically favorable: material of the galaxy flows inward, lowering E .

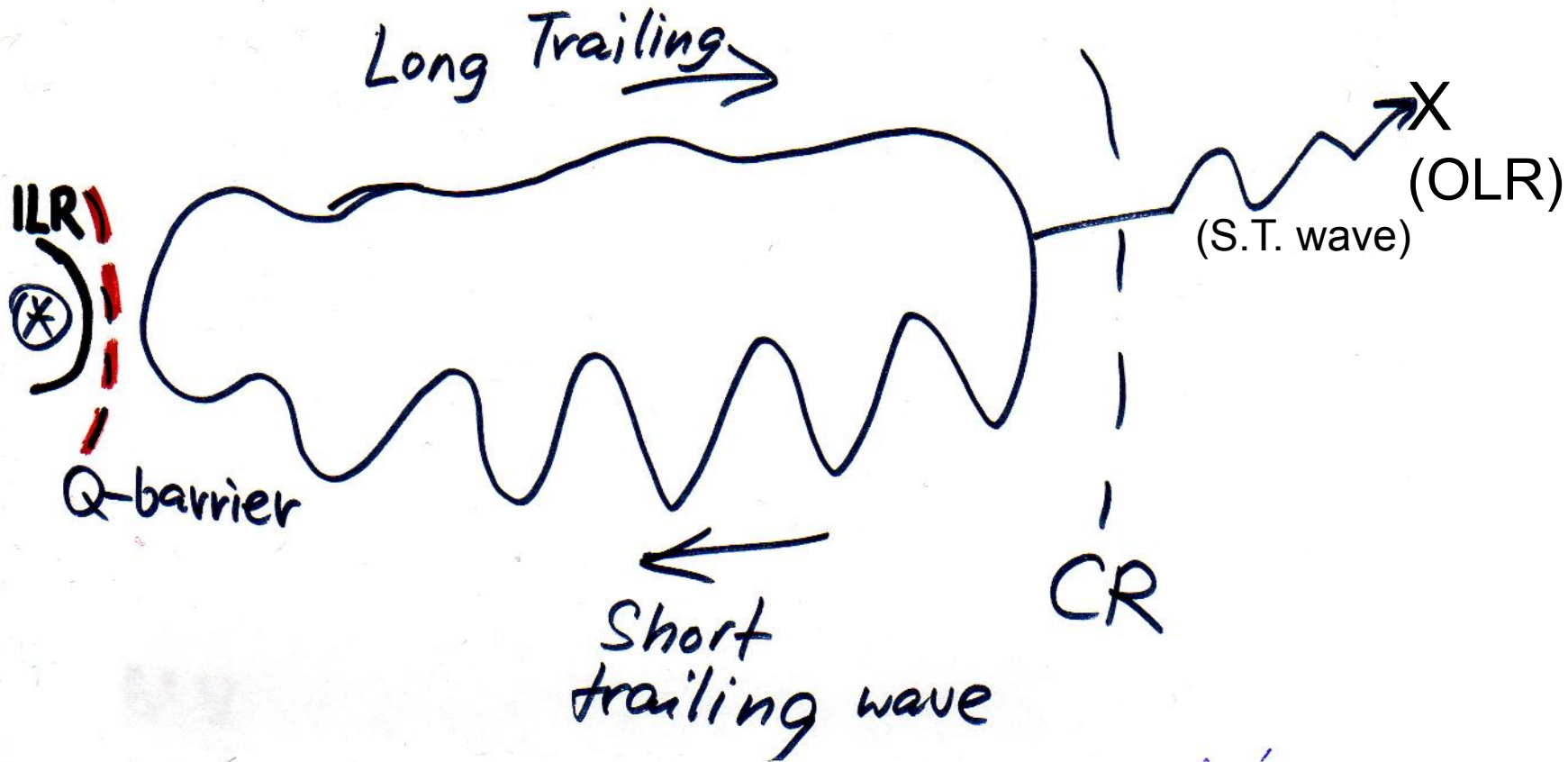
The first type of amplification scenario, called SWING, applies only to **galaxies without ILR**



Peter Goldreich
(Caltech) -
contemporary
astrophysicist and
top dynamicist

This is the **SWING** amplification mechanism (non-WKB) proposed by Goldreich and Lynden-Bell (1965). The S.T. wave arriving at the center passes through and reverses the sense of trailing (trailing to leading), providing positive feedback for the interesting *corotational wave amplifier*. The leading wave swings into a trailing one, and over-reflects by a *large* factor, to satisfy the conservation laws; a 3rd wave is sent “tunneling” through the evanescent zone surrounding CR, toward an OLR. (The Outer wave is weak.)

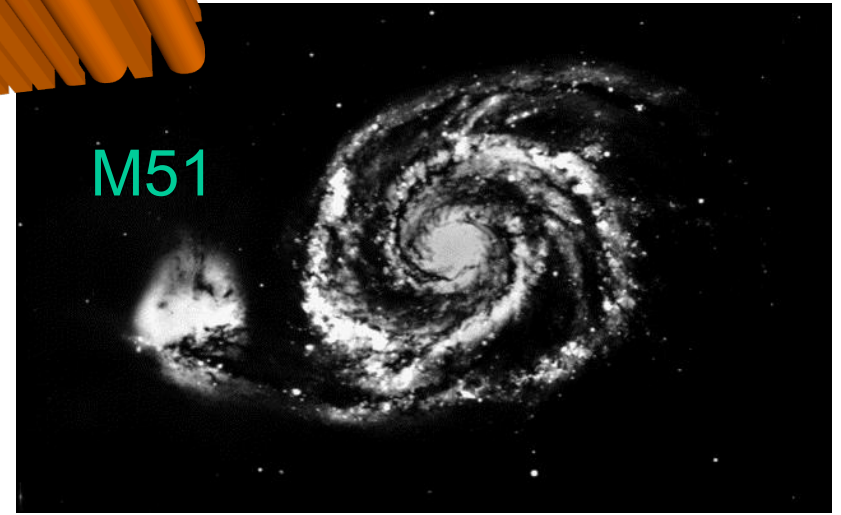
The **WASER** amplification and cycle of waves in Lin-Shu theory (amenable to WKB analysis. **WASER** creates weaker spirals in Sa-Sb spirals) ILR is present, but shielded from the resonant cavity by the so-called Q-barrier, where high values of Safronov-Toomre Q parameter cause a rapid refraction (turning away) of incoming waves.



The over-reflection factor at CR zone is smaller than in SWING, and the stellar waves are growing to only ~5% amplitude (or density contrast)

About 1/3 of spiral galaxies are very regular (grand design spirals)

SWING, encounters



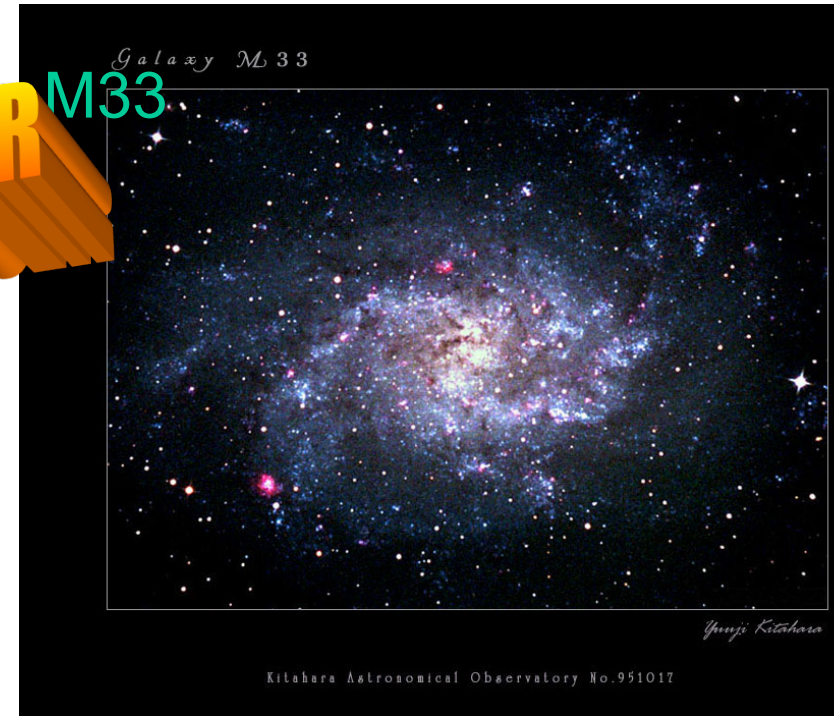
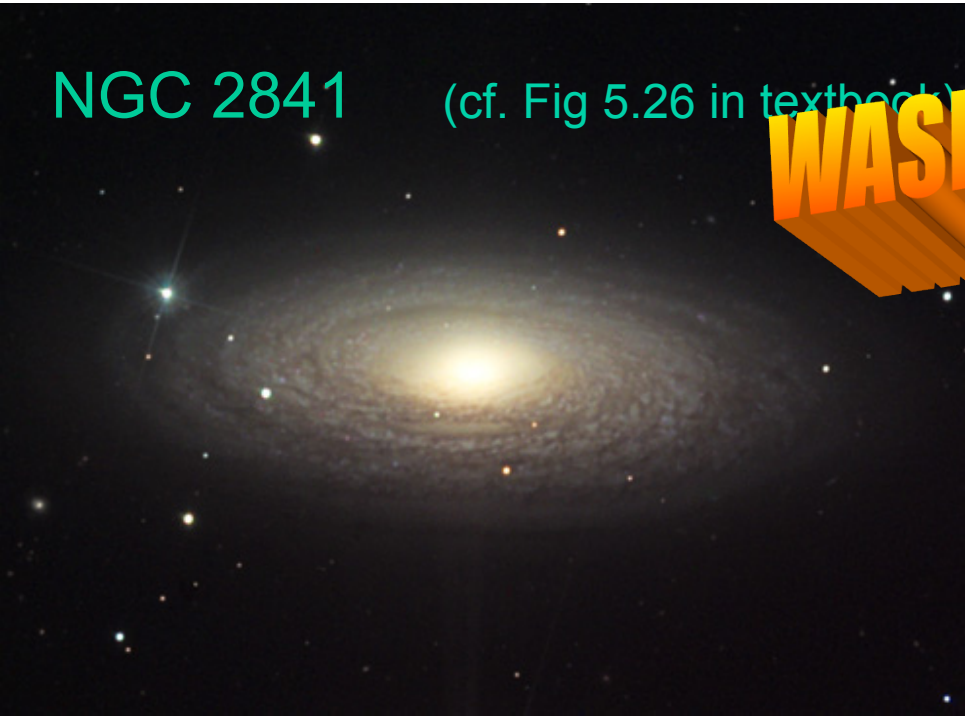
but most galaxies are flocculent, with short, torn arms

NGC 2841

(cf. Fig 5.26 in textbook)

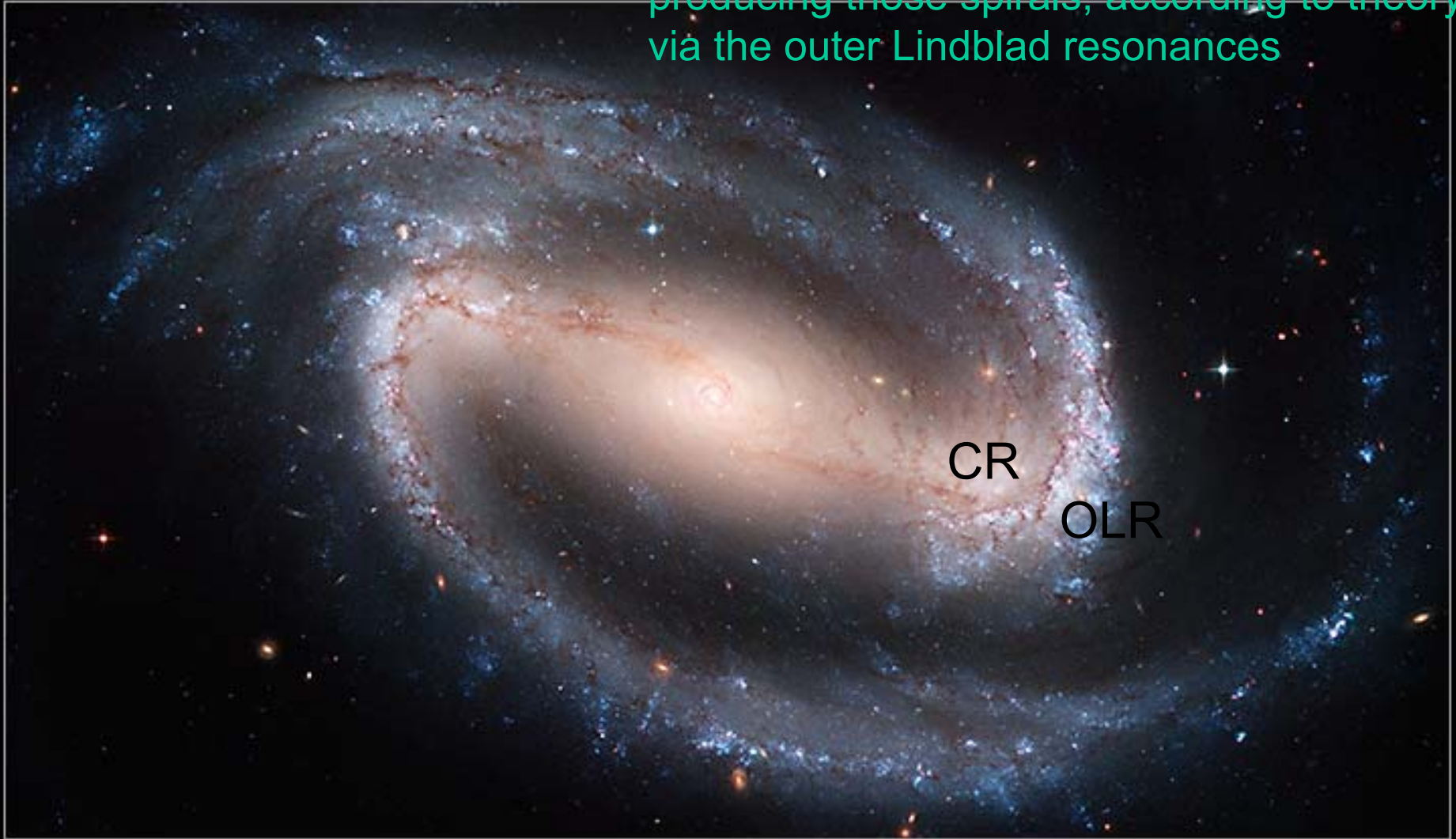
M33

WASER



Barred Spiral Galaxy NGC 1300

Most barred galaxies show regular spirals, often attached to the bar's ends. Bars are producing those spirals, according to theory, via the outer Lindblad resonances



Summary of the origin of spiral patterns:

**Spiral pattern = Waves + Resonances (resonant cavity)
+ Wave amplification + Feedback**

(or w/o amplification & feedback, if waves are driven by external forces like the gravity of bars or perturbing galaxies during galaxy encounters)

Growing modes - cycles:

WASER amplification scheme: a slow wave growth
(obtained in WKB formalism)

SWING amplification: non-WKB rapid amplification mode

(WKB = short-wavelength approximation, or in other words, tightly wrapped spiral approximation)

Summary of the origin of different spiral patterns:

Growth of spiral patterns (modes of density waves circulating in a disk between the CR and LR resonances) causes the observed spiral patterns

Explanation of clear progression of seemingly unrelated features in Sa---Sb---Sc spiral subtype sequence:

Sa galaxies have bigger bulge → steeply rising rot. curve that turns flat roughly where the bulge ends → WASER → weaker and more tightly wrapped spirals

Sc galaxies have a small bulge & dark matter is more dominant → gradually rising $V(R)$ → SWING → strong and more open spirals

This explains the many correlated characteristics of Sa-Sc Hubble classification (bulge-to-disk ratio, rotation curve, strength and shape of spiral arms, presence of young stars in strong spiral arms)